We thank the editor and the two reviewers for their thoughtful comments and suggestions concerning our research. We made major revisions accordingly. We present our response and changes below. The editor's and the reviewers' comments and suggestions are shown in *italic*. Authors' responses are in **bold**.

Response to Editor:

There are three main reasons for this conclusion:

1) The manuscript lacks important information. Even after reading it several times, it is for example not clear to me

• If and how the surface measurements were sampled in time to match the overpass of the OMI data

• If and how the OMI data were sampled in space to match the surface data

We only used the OMI pixels which cover the corresponding AQS sites. The in situ NO_2 data are temporally interpolated based on the overpassing time of the corresponding OMI pixels. We now clarify this in Section 3:

"We group the analysis results into different regions: (a) West, (b) Midwest, (c) Northeast, and (d) South (Fig. 1), following the regional divisions by the United States Census Bureau. To make a fair comparison between the in situ and OMI-based trends, we only use spatially and temporally coincident in situ and OMI NO_2 observations in Section 3.1. The AQS data are temporally interpolated based on the overpassing time of the available OMI pixels which cover the corresponding AQS sites. Similarly, only OMI pixels covering the corresponding available AQS sites are used. The data from each dataset are then aggregated and averaged on a regional basis into time series to calculate the regional trends."

• Whether a constant row filter removing rows 26-55 was used or if the (time dependent) flagging in the DOMINO product was used (both is stated in the text).

We use a constant row filter removing rows 1-5 and rows 26-60 in the analysis. We now clarify this in Section 2.3.1:

"For trend and other analyses of OMI tropospheric VCDs, the data of anomalous pixels must be removed. The row anomaly initially occurred in June 2007 and subsequently in later years affected rows 26-40 (Schenkeveld et al., 2017). Additional anomalies can be found in some years in rows 41-55. For trend analysis from 2005-2014, we exclude rows 26-55, consistent with our understanding of the row anomaly (Schenkeveld et al., 2017) ~~and following the flagging in the DOMINO v2 data product~~. In addition, the data of coarse spatial resolution from rows 1-5 and rows 56-60 are also excluded, as suggested by Lamsal et al. (2015). The selection of rows 6-25 used in this research is stricter than the data flags in the DOMINO v2 product. Furthermore, we exclude OMI data with cloud fraction > 0.3 to minimize retrieval uncertainties due to clouds and aerosols (Boersma et al., 2011; Lin et al., 2014)."

• How exactly the drift over the ocean was accounted for in the data analysis

We calculate the influence of ocean trend (drift) for each year and subtract it from OMI tropospheric SCDs in the data analysis. We now clarify this in Section 2.3.1:

"However, removing this background ocean (absolute) trend has a non-negligible effect in reducing the OMI relative trend (Fig. 1). We treat this trend as a systematic bias. We calculate the contribution from the ocean (absolute) annual trend to SCDs for each year and we subtract it from OMI tropospheric NO_2 SCDs uniformly in the following analysis. Since the origin of this trend is not yet clear, the ocean trend removal method may need updates in future studies."

• Which version of the AMF lookup table was used (you make reference to a recent paper by Lorente et al. for DAK but it is not clear if you use the DOMINO LUT or a more recent version from the QA4ECV project)

We use the DOMINO LUT and we update the reference in Section 2.3:

"As the vertical distribution of NO_2 is usually unknown, we typically substitute x_l by an a priori profile ($x_{l,apriori}$) from a CTM. AMF_l is the sensitivity of NO_2 SCD to VCD at a given altitude (Eskes and Boersma, 2003), and is computed using the Double Adding KNMI (DAK) RTM (Boersma et al., 2011~~Lorente et al., 2017~~)."

2) The explanations given in the manuscript for some of the observed effects are unclear or not convincing:

• The offset correction using data over the ocean is an interesting idea and is in fact used in many satellite data products. However, here the tropospheric slant column is used, which is the result of subtracting the assimilated stratospheric NO2 column from the retrieved slant column. Any global drift in the OMI NO2 slant column data would be absorbed by the data assimilation. The remaining (very small) drift is probably indicative of some problems in the stratospheric correction which would also explain the large variability (note that even negative columns occur in some months) and is certainly not representative for offsets in NO2 slant columns over all of the US. This is the reason why the authors do not apply monthly corrections which they should if they would trust the offset correction approach.

As stated previously, we now state in the paper that "…the origin of this trend is not yet clear…**". The exact origin of the ocean trend is unknown and needs further investigation. We consider the ocean trend to be a systematic bias and we remove this ocean trend in our analysis. We now emphasize this in Section 2.3.1:**

"…This trend may reflect~~s~~ the inaccurately simulated stratospheric SCDs (A. Richter, personal communication, 2018) or the increase in the magnitude of the stripes (step-wise SCD variability from one row to another) in time, which originates from the use of a constant (2005-averaged) solar irradiance reference spectrum in the DOAS spectral fits throughout the mission and the weak increase of noise in the OMI radiance measurements (K. F. Boersma, personal communication, 2017; Zara et al., 2018)… However, removing this background ocean (absolute) trend has a non-negligible effect in reducing the OMI relative trend (Fig. 1). We treat this trend as a systematic bias. We calculate the contribution from the ocean (absolute) annual trend to SCDs for each year and we subtract it from OMI tropospheric NO_2 SCDs uniformly in the following analysis. Since the origin of this trend is not yet clear, the ocean trend removal method may need updates in future studies."

As stated in Section 2.3.1, the results using monthly corrections yield similar results and same conclusions. We add Figures S2 and S3 in the supplement, i.e. the monthly ocean trends and Figure 7 replotted using data with monthly corrections. The monthly ocean trends are calculated using the Mann-Kendall method and are large during SON and DJF (2.0 to 5.2 x10^{13} molecules cm^{-2} yr^{-1}) and small during MAM and JJA (-0.6 to 1.1 x10^{13} molecules cm^{-2} yr^{-1}). The use of the monthly corrections and yearly corrections lead to the same conclusions, as illustrated partly by comparing Figure S3 and Figure 7. We use the (absolute) annual VCD corrections in the manuscript.

We feel the editor has a good point on the unknown nature of the ocean VCD trend, we added in the conclusions section: "Among the corrections, the background ocean trend removal is not as significant as the latter two. Since the origin of this trend is not yet clear, the ocean trend removal method may need updates in future studies.**"**

• The explanation given for the offset trend (increased striping) does not make sense for two reasons: First, striping is by definition deviation from the mean value and thus should not contribute to a drift in the mean, and second, I assume that the authors use destriped data (but also this information is not given in the manuscript).

Our coauthor K. F. Boersma suggested that striping could be the reason for the background ocean trend. He indicated that the increasing deviation from the mean (striping) might lead to a biased ocean trend from using a constant solar radiance spectrum in the DOAS spectral fitting (K. F. Boersma, personal communication, 2017). The section is changed to:

"This trend may reflect~~s~~ the inaccurately simulated stratospheric SCDs (A. Richter, personal communication, 2018) or the increase in the magnitude of the stripes (step-wise SCD variability from one row to another) in time, which originates from the use of a constant (2005-averaged) solar irradiance reference spectrum in the DOAS spectral fits throughout the mission and the weak increase of noise in the OMI radiance measurements (K. F. Boersma, personal communication, 2017; Zara et al., 2018)."

As indicated in the response above, we do not know the exact nature of this trend. We use the OMI data without destriping through the analysis. We now clarify this in Section 2.3:

"We retrieve the tropospheric NO_2 VCDs using the tropospheric slant column densities (SCDs, without destriping) from the Royal Dutch Meteorological Institute (KNMI) Dutch OMI NO_2 product (DOMINO v2, Boersma et al., 2011)."

• The albedo trend correction is an interesting result, but little is said about what the reasons for the differences between MODIS and TEMIS albedo values are. It also is not clear to me if MODIS albedo trends of the order of 0.5% per year are significant.

We focus on the relative trends instead of the absolute values of the albedo values. The albedo data used in original OMI DOMINO v2 product incorporates a climatology dataset with snow/ice albedo adjustment (Section 2.3.2). As a result, DOMINO v2 albedo exhibits no trends in places without snow/ice such as the West and the South (Figure 5). The snow/ice albedo adjustment raises the albedo to 0.6 for pixels whenever and wherever snow is detected by NISE dataset. Therefore, the discrepancies between two albedo datasets mainly come from: (1) the temporal variations of albedo (climatology data from DOMINO v2 vs 16-day data by MODIS); (2) the albedo in case of snow or ice (snow/ice adjustment by DOMINO v2 vs the observations by MODIS). We now clarify this in Section 3.1.2, as follows:

"The OMI DOMINO v2 incorporates a climatology albedo dataset (Kleipool et al., 2008) with snow/ice albedo adjustment ~~using~~, in which the albedo value is reset to be 0.6 if snow/ice is reported in the NASA Near-real-time Ice and Snow Extent (NISE) dataset (Boersma et al., 2011). The climatology albedo data ~~exhibit~~ have no trends. Thus, the trends of albedo from the DOMINO v2 product mainly originate from the yearly variation of NISE detected snow/ice and to a lesser extent the OMI sampling variation. The noticeable seasonal trend of the OMI DOMINO v2 albedo dataset is the 3.9% yr^{-1} increase in DJF of the Midwest and a smaller DJF increase (1.0%) of the Northeast. In contrast, the MODIS albedo dataset exhibits a smaller positive DJF trend (0.8% yr^{-1}), 3.1% yr^{-1} less than the trend from DOMINO v2, in the Midwest, and a small negative DJF trend (-0.8%) in the Northeast. These differences suggest that using a fixed snow/ice albedo and climatology albedo data are inadequate. The comparison to the AQS data shows that the MODIS albedo update leads to better agreement between satellite and in suit trends in winter in these regions (Fig. 4)."

The differences between relative trends of the two albedo datasets in the West and the South are about 0.5-1% yr^{-1}. These differences could result from the temporal variation of surface albedo and do not contribute significantly to the differences between relative trends of OMI and AQS NO_2, as shown in Figure 4. The differences between two albedo datasets in the Midwest and the Northeast mainly come from the inaccurate snow/ice albedo adjustments and are most significant during DJF (Figure 4).

• The lightning filter makes a lot of sense if satellite and surface observations are to be compared. However, the results are puzzling and in contrast to the conclusions drawn in the manuscript: As is evident from Table 1, surface station trends are more affected by the lightning filter than OMI data with the exception of the West, where only little lighting is found over the regions having NO2 above the threshold of 1E15 molec/cm2. The clear improvement in consistency of the two data sets in the South when applying the filter is mainly the result of a change in in-situ trend! In that sense, the lightning filter is more a filter on the surface data than on the OMI data. This result points at sampling issues in the surface data, not inadequacy of the standard OMI product.

We agree that the lightning filter is most useful when comparing trends from the two datasets. We now state it clearly in the abstract: "We recommend future studies to apply these procedures (ocean trend removal and MODIS albedo update) to ensure the quality of satellite-based NO2 trend analysis~~, especially~~ and apply the lightning filter in ~~regions without reliable long-term~~ studying surface NOx emission changes using satellite observations and in comparison with the trends derived from in situ NO_2 measurements."

The lightning filter affects the sampling of AQS data as well as the OMI data. A similar effect can be seen when comparing AQS data with corresponding OMI data used in the study and all AQS data. It is not surprising since while lightning NOx does not affect surface AQS sites directly, chemical (such as cloud effects on photolysis rates, lifetime of NOx, and the ratio of NO_2/NO) and physical (transport by advection and convection) processes affect surface NO_2 concentrations too. Added in Section 3.2:

"Table 1 shows the effects of data sampling when both AQS and OMI data are analyzed and when the lightning filter is applied."

3) The underlying assumption of the whole manuscript is, that trends of surface NO2 in-situ observations should agree with OMI NO2 column trends. As both reviewers point out, this appears to be an apple and oranges comparison, and while it is interesting to compare these two trends, it is by no means clear that they should be exactly the same. As in part pointed out in the manuscript, there are several reasons why they could be different, including representativity of the measurement location (see Fig. 9), vertical NO2 distribution, non-linearity of NOx chemistry and different sensitivity to changes in boundary layer height.

In my personal opinion, the better agreement between surface in-situ trends and the OMI trends after applying the corrections you suggest is a) a coincidence and b) not significant within the uncertainties of the method and the comparison.

We agree that the relative trends from NO_2 VCDs and surface concentrations should not be exactly the same considering the different spatial sampling, inherent difference between trends from NO_2 tropospheric VCDs and surface concentrations, chemical non-linearity, effects of emission changes on NO_2 profiles and etc. The focus of this research is to quantify what the difference between relative trends from both datasets are and how the ending results help us understand the surface emission changes. To avoid confusion, we change our title to "Comparing OMI-based and EPA AQS in situ NO_2 trends: Towards understanding surface NOx emission changes**". We modify our manuscript accordingly.**

In order to make this manuscript publishable in AMT, you need to

• Add the missing information and clarify the details of your approach

• Reconsider your discussions, explanations and conclusions in view of the comments made by the reviewers and listed above (or convince me that I have not understood your arguments)

• Rephrase the manuscript in order not to oversell the achieved improvement in consistency as proving that your corrected OMI time series is more correct than the original one, unless you can show that this is the case.

We have modified the manuscript as suggested.

Response to Referee #1:

Also, I very strongly disagree with the authors' comment that "All observation data need to be corrected when they are used for trend analysis." In its generalness, this is not scientific, in my opinion. This is only the case if one wants to extract information from measurements that was not originally measured, such as comparing apples and oranges. Also, the manuscript still leaves the impression that it is "wrong" of the OMI VCD trends to not be identical to the in-situ measurement network trends, which is still a comparison of apples and oranges in my view.

We made substantial changes to the manuscript as described in the responses to the Editor's questions and believe that we addressed the reviewer's main concern.

Response to Referee #2:

The NO2 concentrations measured at the surface monitors can be substantially different for the sites very close (e.g., 500 m). The size of OMI swath is 24 km x 13 km at the finest resolution and is often larger than this. In addition to differences in the spatial resolution, there are uncertainties in the satellite NO2 retrievals and surface measurements. The trends of OMI tropospheric NO2 columns and those of NO2 measured at surface monitor can be similar as shown in the previous publications. But reconciling the differences between OMI and EPA AQS NO2 trends for large regions can not be a measure for improvement of OMI NO2 retrievals and their trends.

We made substantial changes to the manuscript as described in the responses to the Editor's questions and believe that we addressed the reviewer's concern.

Overall, the manuscript needs a major revision if the authors would like to publish it at AMT. I list my suggestions below.

(1) Authors need to make their focus clear. OMI data co-located with the AQS are mainly discussed through the manuscript, but all of sudden the trends of OMI NO2 for large regions are emphasized (e.g., abstract line 27-31). The comparison of the trends of OMI NO2 for large regions with the trends from the AQS does not make sense. It is confusing if the authors mention the OMI trends at the AQS or the OMI trends for large regions such as West, Midwest etc for all the figures and the text.

Table 1 shows the effects of sampling for regional trends. For comparison purposes, we need to use co-located data; but for understanding regional trends, we need to use all data. For readers interested in satellite data applications, they would be interested in co-located data. But general readers they would be interested in the trends of all data.

(2) Please make careful statements based on clear or enough proofs. The authors added "However, the current OMI tropospheric NO2 retrievals are not designed for analyzing multi-year tropospheric NO2 trends". I do not understand what it actually means. Does it mean the previous publications on OMI NO2 trends are not correct?

We removed this sentence.

(3) The ocean trends do not look significant as another colleague mentioned. Albedo correction based on MODIS data looks promising as Russell et al. (2011) demonstrated. Lightning filtering also gives new insights for southern US. It is important to show spatial variability of the trends or NO2 columns from adopting MODIS albedo and lightning filtering similar to Figure 8. Detailed spatial distribution rather than the simple values for 4 large districts would be useful. Add explanations of why the impact of lightning filtering is large for the Northeast US (not only the South US, see Figure 1).

We now state in the manuscript that the effects of removing ocean trends are not as large as albedo and lightning filter processing. We present Figure R1 here with the spatial distributions of OMI-based NO_2 trends of the standard product and the three variants.

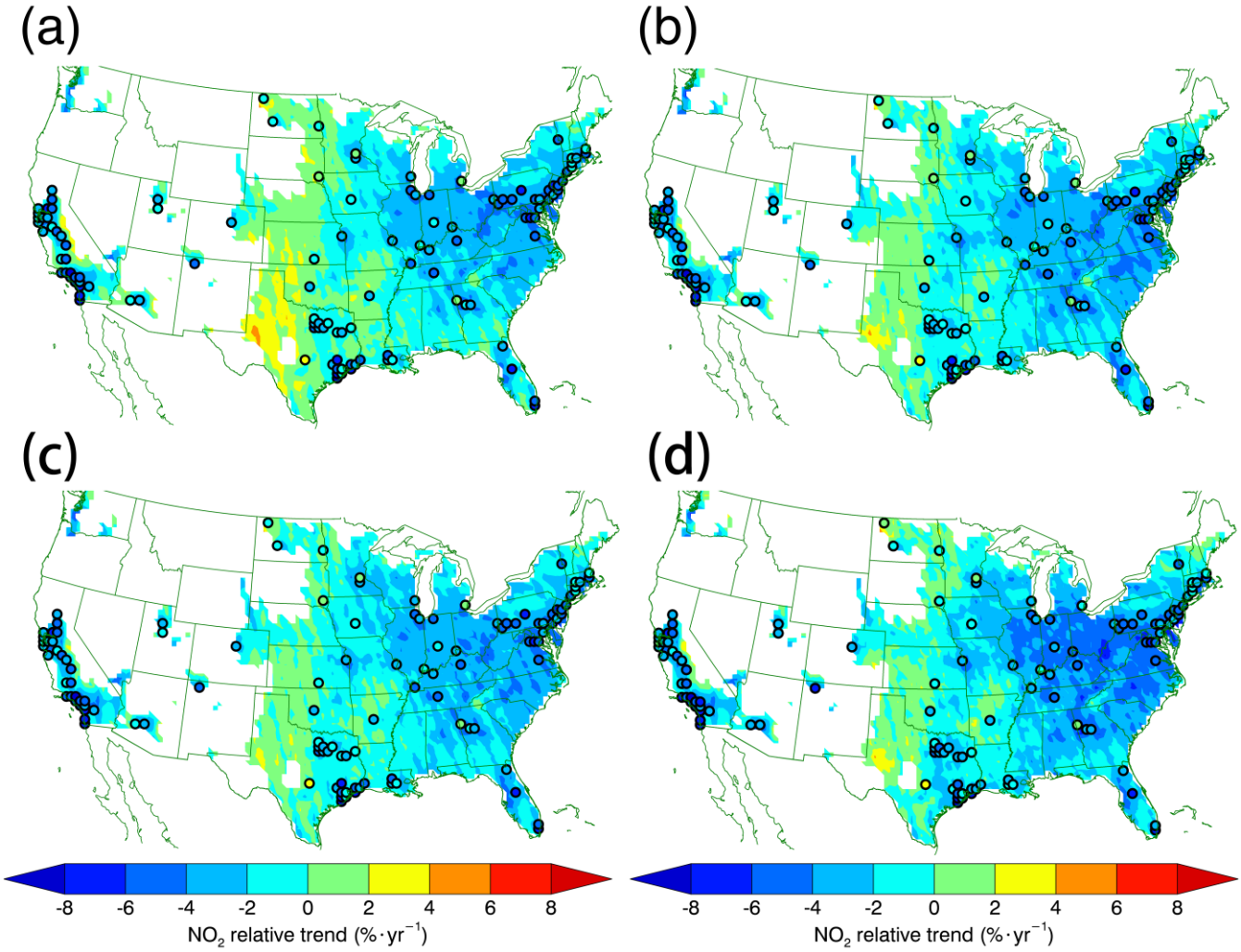

Figure R1: Annual relative trends of OMI-based NO_2 for "Standard" (a), "Ocean" (b), "MODIS" (c), and for "Lightning filter" (d) as the colored background. Black bordered circles indicate corresponding AQS NO_2 trends. Grid cells with 2005-2014 mean NO_2 VCDs < $1x10^{15}$ molecules cm^{-2} are excluded in the analysis and are shown in white.

The Northeast U.S. can be affected by lightning NOx transported from the South. We design the lightning filter such that we screen the data affected by transported lightning NOx from the South to the Northeast. We have stated in Section 2.3.3, "While there are fewer lightning flashes in the Northeast than the South (Fig. 3), large amounts of lightning NOx can be produced by high flash ratios of severe thunderstorms and they can be transported northward from the South to the Northeast (Choi et al., 2005). We therefore further filter OMI NO_2 data in the Northeast on the basis of CG lightning flash rates in the South. If the average CG flash rate in the South exceeds the 95th percentile value of the NLDN observations, which is 0.035 flash km^{-2} day^{-1} (Fig. S2 in the Supplement), we exclude in the analysis the Northeast OMI data in the following 72 hours." **We add the following clarification in Section 3.1.3:**

"Fig. 6 shows that the lightning filter significantly reduces the difference between the OMI-based relative trend and that of the AQS data by 0.5-1.4% yr^{-1} in the Northeast and 0.9-1.3% yr^{-1} in the South. As a result, the seasonal trend differences are within 0.9% yr^{-1} in these two regions except during SON. The Northeast is affected by the lightning filter due to lightning in this region and transport of lightning NOx from the South (Section 2.3.3)."

(4) Referring to Lamsal et al. (2015), the authors only mentioned average values. Lamsal et al. (2015) also stated that the impact of changing anthropogenic emissions in calculating a priori profiles can be large up to 15% more reductions in the declining trend depending on the location. Lamsal et al. used 1 degree x 1.25 degree GMI model grid resolution to produce trace gas profiles. The authors have the REAM model setting with the 36 km resolution and are capable of producing own profiles rather than fully

depending on discussions in the previous publication. I am not convinced with lines 28- 29, page 4, "The NO2 VCD trend analysis is particularly sensitive to the first two factors and we will discuss these in the following sections".

Lamsal et al. (2015) illustrated in the Figure 3 of the referenced publication that the difference in reduction is generally less than 2% in NO_2 abundant regions during 2005-2010 (equivalent to 0.3% yr^{-1}). On a regional basis, it is difficult that the a priori profile can have a significant effect on the relative trends. As reported in a newly published study, the reduction of emission may have slowed down after 2010 (Jiang et al., 2018). This would lead to an even smaller contribution from NOx emission changes to NO_2 trend during the studied period of 2005-2014. To fully quantify the emission changes, inverse modeling of NOx emission over a 10-year timespan is needed.

We update the manscript as below:

"~~We find that the NO_2 VCD trend analysis is particularly sensitive to the first two factors~~ In this study, we find that the first two factors are essential in NO_2 VCD trend analysis and we will discuss these in the following sections."

(5) Discrepancies between NO2 chemiluminescence to photolytic converter measurement are small in the morning (7-9 am) and become larger in the afternoon. The plots of diurnal variations of the ratios at each station would give a confidence in the quality of the measurements.

We have stated in Section 2.1, "In this study, we only examine the relative trends and therefore the analysis results are not affected by the uncertainties in the in situ NO_2 measurement corrections.". **Due to data availability, only one site has more than one year of consecutive data with both measurements. We show the averaged diurnal cycle of ratios in Figure R2, as below.**

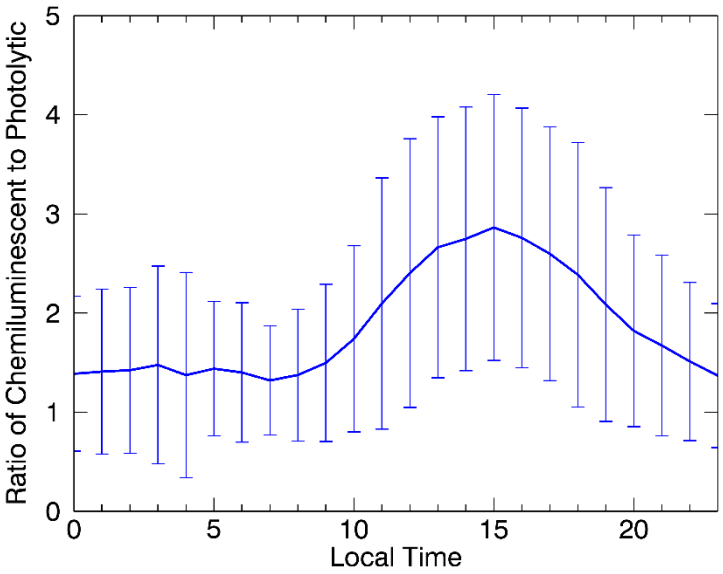

Figure R2. The diurnal cycle of ratios between NO_2 surface concentrations of chemiluminescent to photolytic instruments in Sacramento, CA. The errorbars represent standard deviations.

(6) I do not understand the meaning of Figure 9. Is this for the apple-orange comparison of the trends from the AQS and those from OMI data for the large areas?

Figure 9a shows the "Lightning filter" OMI-based NO_2 relative trends as a function of averaged NO_2 VCDs. Figure 9b shows the averaged NO_2 VCDs across U.S. Figure 9 intends to help readers understand that the NO_2 reduction is larger in NO_2 abundant areas where most AQS sites are located. For general readers, they will want to understand how the regional trends of OMI data compare to AQS data. We show that the difference is very large and explain the reasons.

REFERENCES

Jiang, Z., McDonald, B. C., Worden, H., Worden, J. R., Miyazaki, K., Qu, Z., Henze, D. K., Jones, D. B. A., Arellano, A. F., Fischer, E. V., Zhu, L., and Boersma, K. F.: Unexpected slowdown of US pollutant emission reduction in the past decade, Proceedings of the National Academy of Sciences, 10.1073/pnas.1801191115, 2018.

~~Reconciling the differences between~~Comparing OMI-based and EPA AQS in situ NO_2 trends: Towards understanding surface NOx emission changes

Ruixiong Zhang[1], Yuhang Wang[1], Charles Smeltzer[1], Hang Qu[1], William Koshak[2], K. Folkert Boersma[3,4]

[1]School of Earth and Atmospheric Sciences, Georgia Institute of Technology, Atlanta, Georgia, USA
[2]NASA-Marshall Space Flight Center, National Space Science & Technology Center, 320 Sparkman Drive, Huntsville, Alabama, USA
[3]Meteorology and Air Quality Group, Wageningen University, the Netherlands
[4]Royal Netherlands Meteorological Institute, De Bilt, the Netherlands

Correspondence to: Yuhang Wang (yuhang.wang@eas.gatech.edu)

Abstract. With the improved spatial resolution than earlier instruments and more than ten years of service, tropospheric NO_2 retrievals from the Ozone Monitoring Instrument (OMI) have led to many influential studies on the relationships between socioeconomic activities and NOx emissions. ~~However,~~Previous studies have shown that the ~~current~~ OMI ~~tropospheric~~ NO_2 ~~retrievals are not designed for analyzing multi-year tropospheric NO_2~~data show different relative trends~~.~~ compared to in situ measurements. However, the sources of the discrepancies need further investigations. This study focuses on how to ~~improve~~appropriately compare relative trends derived from OMI ~~NO_2 retrievals for more reliable trend analysis~~and in situ measurements. We retrieve OMI tropospheric NO_2 vertical column densities (VCDs) and obtain the NO_2 seasonal trends over the United States, which are compared with coincident in situ surface NO_2 measurements from the Air Quality System (AQS) network. The Mann-Kendall method with the Sen's slope estimator is applied to derive the NO_2 seasonal and annual trends for four regions at coincident sites during 2005-2014. The OMI-based NO_2 seasonal relative decreasing trends are generally biased ~~high~~low compared to the in situ trends by up to 3.7% yr^{-1}, except for the underestimation in the Midwest and Northeast during Dec-Jan-Feb (DJF). We improve the OMI retrievals for trend analysis by removing the ocean trend, using the MODerate-resolution Imaging Spectroradiometer (MODIS) albedo data in air mass factor (AMF) calculation~~, and applying.~~ We apply a lightning flash filter to exclude lightning affected ~~OMI NO_2 retrievals.~~data to make proper comparisons. These ~~improvements~~data processing procedures result in close agreement (within 0.3% yr^{-1}) between in situ and OMI-based NO_2 regional annual relative trends. The ~~derived OMI-based annual regional NO_2~~ remaining discrepancies may result from inherent difference between trends ~~change by a factor~~ of ~~> 2 for the South, the Midwest,~~NO_2 tropospheric VCDs and ~~the West~~surface concentrations, different spatial sampling of the measurements, chemical non-linearity, and ~~seasonal~~tropospheric NO_2 profile changes ~~can be even larger.~~ We recommend future studies to apply these procedures (ocean trend removal and MODIS albedo update) to ensure the quality of satellite-based NO_2 trend analysis~~, especially~~ and apply the lightning filter in ~~regions without reliable long-term~~studying surface NOx emission changes using satellite observations and in comparison with the trends

derived from in situ NO_2 measurements. ~~We~~With these data processing procedures, we derive ~~optimized~~ OMI-based NO_2 regional annual relative trends using all available data for the West (-2.0%±0.3 yr^{-1}), the Midwest (-1.8%±0.4 yr^{-1}), the Northeast (-3.1%±0.5 yr^{-1}), and the South (-0.9%±0.3 yr^{-1}). The OMI-based annual mean trend over the contiguous United States is -1.5%±0.2 yr^{-1}. It is a factor of 2 lower than that of the AQS in situ data (-3.9%±0.4 yr^{-1}); the difference is mainly due to the fact that the locations of AQS sites are concentrated in urban and suburban regions.

1 Introduction

Nitrogen dioxide (NO_2) is an air pollutant. At high concentrations, it aggravates respiratory diseases and can lead to acid rain formation (e.g., Lamsal et al., 2015). It is also a key player to produce another pollutant, ozone (O_3), through photochemical reactions in the presence of Volatile Organic Compounds (VOCs) under sunlight. Tropospheric NO_2 is emitted both anthropogenically and naturally (e.g., Gu et al., 2016). Anthropogenic fossil fuel combustions and biomass burnings emit mostly nitrogen monoxide (NO) under high temperature, which is later oxidized by O_3 into NO_2. Major natural NO_2 sources include lightning and soils.

Surface NO_2 concentrations are regulated by the U.S. Environmental Protection Agency (EPA) through the National Ambient Air Quality Standards (NAAQS). NO_2 is measured routinely at the EPA Air Quality System (AQS) sites (Demerjian, 2000). Although the AQS network continually provides valuable hourly NO_2 measurements, AQS sites are mostly located in urban and suburban regions, leaving large regions of rural areas unmonitored. Satellite data provide a better spatial coverage than the in situ measurements.

Several satellites were launched to monitor tropospheric NO_2 vertical column densities (VCDs), such as the SCanning Imaging Absorption spectroMeter for Atmospheric CHartographY (SCIAMACHY), the Global Ozone Monitoring Experiment–2 (GOME-2), and the Ozone Monitoring Instrument (OMI). For trend analysis, the tropospheric NO_2 products from OMI surpass the others for a relatively high spatial resolution and over one decade of continuous operation (Boersma et al., 2004; Boersma et al., 2011). Thus, OMI NO_2 retrievals are widely applied in NO_2 and NOx emission trend studies (e.g., Lin et al., 2010, 2011; Castellanos et al., 2012; Russell et al., 2012; Gu et al., 2013; Lamsal et al., 2015; Lu et al., 2015; Tong et al., 2015; Cui et al., 2016; Duncan et al., 2016; de Foy et al., 2016a, 2016b; Krotkov et al., 2016; Liu et al., 2017). Tong et al. (2015) reported that the reduction rates calculated from OMI NO_2 VCDs and AQS surface NO_2 data at eight cities were -35% and -38% from 2005 to 2012, respectively. Lamsal et al. (2015) also found the divergence between the annual trends inferred from the two datasets, i.e. -4.8% yr^{-1} vs -3.7% yr^{-1} during 2005-2008, and -1.2% yr^{-1} vs -2.1% yr^{-1} during 2010-2013. There are several potential factors attributing to the discrepancies between trends from satellite and ground-based measurements: interferences by the oxidation products of NOx from the chemiluminescent instruments (Lamsal et al., 2008, 2014, 2015), the differences of sampling time between OMI (~13:30 local time) and AQS (hourly) measurements (Tong et al., 2015), a high sensitivity of NO_2 VCDs to high-altitude NO_2 in contrast to the high sensitivity of surface NO_2 concentrations

to surface NOx emissions (Duncan et al., 2013; Lamsal et al., 2015), spatial representativeness of satellite pixels (Lamsal et al., 2015), and high uncertainties of satellite retrievals in clean regions (Lamsal et al., 2015).

To understand how various factors and the retrieval procedure affect the ~~resulting~~differences between the OMI derived trends and ~~their differences from~~ those derived from the surface AQS measurements, we utilize a regional 3-D chemistry transport model (CTM), a radiative transfer model (RTM), and the Mann-Kendall method (Mann, 1945; Kendall, 1948) to calculate OMI-based NO_2 seasonal relative trends during Dec-Jan-Feb (DJF), Mar-Apr-May (MAM), Jun-Jul-Aug (JJA), and Sept-Oct-Nov (SON) (Section 2). ~~To reconcile with the AQS based regional NO_2 trends, we~~We find that ~~three~~two procedures are essential to ensure the quality of trend analysis using OMI tropospheric NO_2 VCDs, including the ocean trend removal~~,~~ and the MODerate-resolution Imaging Spectroradiometer (MODIS) albedo update in calculating the air mass factors (AMFs~~), and the~~). The lightning filter (Section 3.1~~).~~) is necessary for comparing OMI-based and in situ AQS NO_2 trends. With these procedures implemented, the differences between OMI-based and AQS in situ annual relative trends are within 0.3% yr^{-1} of coincident measurements for all the four regions. Finally, we estimate the OMI-based annual relative trends across the nation in Section 3.2. Conclusions are given in Section 4.

2 Methods

2.1 EPA AQS surface NO_2 measurements

The in situ surface NO_2 measurements from the U.S. EPA AQS network are used in this research. Sites with a continuous measurement gap of more than 50 days are removed and the observations of 140 remaining cites are used (Fig. 1). The AQS chemiluminescent analyzers are equipped with molybdenum converters to measure ambient NO_2 concentrations. These analyzers are known to have high biases, since the converters are not NO_2 specific and they measure some fractions of peroxyacetyl nitrate, nitric acid and organic nitrates (Demerjian, 2000; Lamsal et al., 2008). In addition to chemiluminescent analyzers, several NO_2 specific photolytic instruments were deployed since 2013. By utilizing the data from both chemiluminescent and photolytic measurements at coincident sites during the overpassing time of OMI, we calculate the observed NO_2 concentration ratio between both measurements in Fig. S1 in the Supplement. The ratio peaks at 2.3 in June and decreases to 1.3 in November, indicating that the chemiluminescent analyzers overestimate by 27%-132% than photolytic instruments. This finding is in agreement with Lamsal et al. (2008). We correct the chemiluminescent NO_2 data by the observed ratio assuming that the inter-annual change is small and the high bias of the chemiluminescent measurements is identical at all sites. This correction may contribute to the differences between in situ and OMI based absolute NO_2 trends but do not significantly affect the relative trends (since the correction is canceled out in computing relative trends). In this study, we only examine the relative trends and therefore the analysis results are not affected by the uncertainties in the in situ NO_2 measurement corrections.

2.2 REAM model

We use a 3-D Regional chEmical trAnsport Model (REAM) in the simulation of NO_2 profiles. REAM has widely been used in atmospheric NO_2 studies, including vertical transport (Choi et al., 2005; Zhao et al., 2009a; Zhang et al., 2016a), emission inversions (Zhao et al., 2009b; Yang et al., 2011; Gu et al., 2013, 2014, 2016), and regional and seasonal variations (Choi et al., 2008a, 2008b). The model has a horizontal resolution of 36 km with 30 vertical layers in the troposphere, 5 vertical layers in the stratosphere, and a model top of 10 hpa. In this study, the domain of REAM is about 400 km larger on each side than the contiguous United States (CONUS). Meteorology inputs driving transport process are simulated by the Weather Research and Forecasting model (WRF) assimilations constrained by National Centers for Environmental Prediction Climate Forecast System Reanalysis (NCEP CFSR, Saha et al., 2010) 6-hourly products. The KF-eta scheme is used for sub-grid convective transport in WRF (Kain and Fritsch,1993). We run the WRF model with the same resolution as in REAM but with a domain 10 grids larger on each side than that of REAM. REAM updates most of the meteorology inputs every 30 minutes while those related to convective transport and lightning parameterization are updated every 5 minutes. The chemistry mechanism expands that of a global CTM GEOS-Chem (V9-02) with aromatics chemistry (Bey et al., 2001; Liu et al., 2010, 2012a, 2012b; Zhang et al., 2017). For consistency, the GEOS-Chem (V9-02) simulation with $2° \times 2.5°$ resolution is used to generate initial and boundary conditions for chemical tracers.

Anthropogenic emissions of NOx and other chemical species are from the U.S. National Emission Inventory 2008 prepared using the Sparse Matrix Operator Kernel Emission (SMOKE) model. Biogenic emissions are simulated online using the Model of Emissions of Gases and Aerosols from Nature (MEGAN) algorithm (v2.1, Guenther et al., 2012). We parameterize lightning emitted NOx as a function of convective mass flux and Convective Available Potential Energy (CAPE) (Choi et al., 2005). NOx production per flash is set to 250 moles NO per flash, and the emissions are distributed vertically following the C-shaped profiles by Pickering et al. (1998). For recent model evaluations of REAM with observations, we refer readers to Zhang et al. (2016a, 2016b), Cheng et al. (2017), and Zhang et al. (2017).

2.3 OMI-based NO_2 VCDs

We retrieve the tropospheric NO_2 VCDs using the tropospheric slant column densities (SCDs, without destriping) from the Royal Dutch Meteorological Institute (KNMI) Dutch OMI NO_2 product (DOMINO v2, Boersma et al., 2011). OMI onboard the Aura satellite was launched in July 2004 and is still active. OMI overpasses the equator at about 13:30 Local Time (LT) and obtains global coverage with a 2600 km viewing swath spanning 60 rows. It has a ground level spatial resolution up to 13 km x 24 km (at nadir). The spatial extent of the OMI pixels will not affect our analysis as we focus on regional trend analysis. SCDs are retrieved by matching a modeled spectrum to an observed top-of-atmosphere reflectance with the Differential Optical Absorption Spectroscopy (DOAS) technique within a fitting window of 405-465nm. The stratospheric portion of SCDs are estimated and subsequently removed with a global CTM TM4 with stratospheric ozone assimilation (Dirksen et al., 2011). Deriving tropospheric VCDs from the remaining tropospheric SCDs requires the calculation of AMFs. Being an optically thin

gas, tropospheric AMF for NO_2 can be calculated from AMF for each vertical layer (AMF_l) weighted by NO_2 partial VCDs at the corresponding layer (x_l) (Boersma et al., 2004), as shown in equation (1).

$$\text{tropospheric AMF} = \frac{tropospheric\ SCD}{tropospheric\ VCD} = \frac{\int AMF_l x_l dl}{\int x_l dl} \quad (1)$$

As the vertical distribution of NO_2 is usually unknown, we typically substitute x_l by an a priori profile ($x_{l,apriori}$) from a CTM. AMF_l is the sensitivity of NO_2 SCD to VCD at a given altitude (Eskes and Boersma, 2003), and is computed using the Double Adding KNMI (DAK) RTM (~~Lorente~~Boersma et al., ~~2017~~2011). As a result, the retrieved tropospheric NO_2 VCD computation depends on the a priori NO_2 vertical profile, the surface reflectance, the surface pressure, the temperature profile, and the viewing geometry (Boersma et al., 2011). Previous studies have addressed the sources of uncertainties in NO_2 retrievals, including surface reflectance resolutions (Russell et al., 2011; Lin et al., 2014), lightning NOx (Choi et al., 2005a; Martin et al., 2007; Bucsela et al., 2010), a priori CTM uncertainties (Russell et al., 2011; Heckel et al., 2011; Lin et al., 2012; Laughner et al., 2016), surface pressure and reflectance anisotropy in rugged terrain (Zhou et al., 2009), cloud and aerosol radiance (Lin et al., 2014, 2015), and boundary layer dynamics (Zhang et al., 2016a). ~~We~~ In this study, we find that the first two factors are essential in NO_2 VCD trend analysis ~~is particularly sensitive to the first two factors~~ and we will discuss these in the following sections.

AMFs are derived using the pre-computed altitude-dependent AMF lookup table, which is generated by the DAK RTM. We use the NO_2 profiles from REAM, temperature and pressure from CSFR, viewing geometry and cloud information from DOMINO v2 product. We use the REAM results of 2010 to avoid the uncertainty introduced by yearly variation of NO_2 profiles. The yearly variations of meteorology and anthropogenic emission changes have little impact in polluted areas on trend analysis results using OMI data (Lamsal et al., 2015). We use the surface reflectance from DOMINO v2 product as default (Kleipool et al., 2008), and update it using a surface reflectance product with a higher temporal resolution (Section 2.3.2). The derived tropospheric NO_2 VCD relative trends with default surface reflectance are referred as "Standard".

2.3.1 Ocean trend removal

For trend and other analyses of OMI tropospheric VCDs, the data of anomalous pixels must be removed. The row anomaly initially occurred in June 2007 and subsequently in later years affected rows 26-40 (Schenkeveld et al., 2017). Additional anomalies can be found in some years in rows 41-55. For trend analysis from 2005-2014, we exclude rows 26-55, consistent with our understanding of the row anomaly (Schenkeveld et al., 2017~~), and following the flagging in the DOMINO v2 data product.~~). In addition, the data of coarse spatial resolution from rows 1-5 and rows 56-60 are also excluded, as suggested by Lamsal et al. (2015). The selection of rows 6-25 used in this research is stricter than the data flags in the DOMINO v2 product. Furthermore, we exclude OMI data with cloud fraction > 0.3 to minimize retrieval uncertainties due to clouds and aerosols (Boersma et al., 2011; Lin et al., 2014).

Fig. 2a shows that there is an apparent increasing trend of the averaged tropospheric SCDs in the remote ocean region (Fig. 2b) with minimal marine traffic. ~~This trend reflects~~This trend may reflect the inaccurately simulated stratospheric SCDs (A. Richter, personal communication, 2018) or the increase in the magnitude of the stripes (step-wise SCD variability from one row to another) in time, which originates from the use of a constant (2005-averaged) solar irradiance reference spectrum in the DOAS spectral fits throughout the mission and the weak increase of noise in the OMI radiance measurements (F. Boersma, personal communication, 2017; Zara et al., 2018). Fig. 2a shows that there is a positive annual trend of $1.75\pm0.45\times10^{13}$ molecules cm^{-2} yr^{-1}. The ocean trend is insensitive to the region selection in the remote North Pacific (varies within 10%). We only analyze OMI tropospheric column trends over the CONUS for grid cells with 2005-2014 averaged VCDs > 1×10^{15} molecules cm^{-2}, which tends to minimize the effect of the background noise. However, removing this background ocean (absolute) trend has a non-negligible effect in reducing the OMI relative trend (Fig. 1). We treat this trend as a systematic bias. We calculate the contribution from the ocean (absolute) annual trend to SCDs for each year and subtract it from OMI tropospheric NO_2 SCDs uniformly in the following analysis. Since the origin of this trend is not yet clear, the ocean trend removal method may need updates in future studies. We refer to such derived (relative) trend data as "Ocean". An alternative method is to subtract monthly ~~SCDs~~SCD trends of the remote ocean region (Fig. S2 in the Supplement) from the OMI tropospheric SCD data. Although the end results (Fig. S3 in the Supplement) are essentially the same as the annual trend removal method, noises are added to the SCD data ~~(Fig. 2a),~~ making it more difficult to understand the effects of the MODIS albedo update and the lightning filter (next sections). We therefore choose to use the (absolute) annual trend removal method here.

2.3.2 MODIS albedo update

The albedo data used to calculate the AMF_l in "Standard" and "Ocean" versions of trend analysis are from the DOMINO v2 products, which are the climatology of averaged OMI measurements during 2005-2009 with a spatial resolution of 0.5°×0.5° (Kleipool et al., 2008) and is valid for 440 nm. We recalculate the AMF_l using the MODIS 16-day MCD43B3 albedo product with 1km spatial resolution, which combines data from both MODIS onboard Aqua and Terra satellites (Schaaf et al., 2002; Tang and Zhang, 2007). Aqua and Terra have an equatorial overpassing time of 13:30 LT and 10:30 LT, respectively. The band 3 (459nm-479nm) is used to match the NO_2 fitting window (405nm-465nm). The albedo is spatially integrated to the geometry of OMI pixels and is temporally interpolated to match OMI overpassing dates. In order to maintain the consistency of the DOMINO retrieval algorithm (Boersma et al., 2011), we only use the MODIS data to improve the temporal variations of albedo data used in the retrieval. We scale the MODIS albedo data such that the mean albedo during 2005-2009 is the same as the OMI climatology at 0.5°×0.5°. We recalculate OMI tropospheric VCDs using the MODIS albedo data as described. We recalculate the relative OMI trend and remove the ocean (absolute) trend (Section 2.3.1). We refer to this version of OMI relative trend data as "MODIS".

2.3.3 Lightning event filter

Over North America, lightning is a major source of NOx in the free troposphere and its simulations in CTMs are uncertain (e.g., Zhao et al., 2009a; Luo et al., 2017). The large temporospatial variations of lightning NOx make it difficult to compute satellite based NO_2 trends by changing the vertical distributions of NO_2 affecting the AMF calculation (e.g., Choi et al., 2008b; Lamsal et al., 2010) and the SCD values. Furthermore, accompanying lightning occurrences, the presence of cloud significantly affects the lifetime of NOx and the partitioning of NO_2 to NO in daytime and convective transport exports NOx from the surface and boundary layer to free troposphere, changing surface and column NO_2 concentrations. Given the difficulty to simulate lightning NOx accurately across different years and meteorological effects (vertical mixing) of lightning, we use a lightning filter to remove potential effects of lightning NOx on the basis of the flash rate observations of cloud-to-ground (CG) lightning flash data detected by the National Lightning Detection Network™ (NLDN) (Cummins and Murphy, 2009; Rudlosky and Fuelberg, 2010). NLDN only reports the ground point of a CG lightning flash, while the CG lightning flash can extend horizontally to tens of kilometers. A CG lightning flash can affect the NO_2 retrievals not only in the model grid cell where the CG lightning is located but also the nearby model grid cells. The atmospheric lifetime of NOx in the free troposphere can be up to 1 week. Therefore, we exclude the OMI NO_2 data within a radius of 90 km of the NLDN-reported CG lightning location (about two model grid cells around the grid cell where the CG lightning is located) for a period of 72 hours after the lightning occurrence. Since lightning usually occur along the track of a thunderstorm, the 90 km radius is more a constraint on lightning NOx effects across the track. The extended period of 72 hours is to ensure that we exclude data affected by lightning NOx. Figure 4 shows the distribution of the number of days of 2005-2014 with lightning detection. The Southwest monsoon and the South regions have more lightning days than the other areas. While there are fewer lightning flashes in the Northeast than the South (Fig. 3), large amounts of lightning NOx can be produced by high flash ratios of severe thunderstorms and they can be transported northward from the South to the Northeast (Choi et al., 2005). We therefore further filter OMI NO_2 data in the Northeast on the basis of CG lightning flash rates in the South. If the average CG flash rate in the South exceeds the 95th percentile value of the NLDN observations, which is 0.035 flash km^{-2} day^{-1} (Fig. ~~S2~~S4 in the Supplement), we exclude in the analysis the Northeast OMI data in the following 72 hours. Excluding the OMI data based on CG lightning data implicitly removes the data affected by cloud-to-cloud lightning collocated with CG lightning. The lightning filter removes about 2%, 27%, 20%, and 19% of OMI data, which are coincident with AQS data, for the West, the Midwest, the Northeast and the South, respectively. We refer to this version of OMI relative trend data as "Lightning filter".

3 Results and discussion

We group the analysis results into different regions: (a) West, (b) Midwest, (c) Northeast, and (d) South (Fig. 1), following the regional divisions by the United States Census Bureau. To make a fair comparison between the in situ and OMI-based trends, we only use spatially and temporally coincident in situ and OMI NO_2 observations in Section 3.1. The AQS data are temporally interpolated based on the overpassing time of the available OMI pixels which cover the corresponding AQS sites. Similarly,

only OMI pixels covering the corresponding available AQS sites are used. The data from each dataset are then aggregated and averaged on a regional basis into time series to calculate the regional trends.

We apply the Mann-Kendall method with the Sen's slope estimator to calculate the relative trend of NO_2 for each season, i.e. DJF, MAM, JJA, and SON, during 2005-2014. We compute the uncertainties of the trends with the 95th percentile confidence intervals using the Mann-Kendall method. Note that when we compare in situ and OMI-based trends, the lightning filter also removes in situ NO_2 data, which are coincident with the OMI NO_2 data affected by lightning. This leads to slightly different in situ NO_2 trends between Fig. 4 and Fig. 6 (Section 3.2.3). We first compute the trends using the "Standard" OMI VCD data. The ocean trend removal, MODIS albedo update, and lightning filter are then added in sequence to compute three different OMI-based NO_2 trends (in addition to "Standard") to compare to the AQS in situ results. A subtlety in the comparison is that the coincident data change when the lightning filter is applied. As a result, the AQS in situ results in this set of comparison differ from those in the other three sets.

3.1 In situ and "Standard" OMI-based trends

Fig. 4 shows that both AQS in situ and "Standard" OMI-based seasonal relative trends are negative for all seasons across the regions. OMI-based trends generally underestimate the decreasing trends by up to 3.7% yr^{-1} (the absolute difference between relative trends) except for the large overestimation in the Midwest and the Northeast regions during DJF. The overestimates in these two regions are 3.0% yr^{-1} and 1.1% yr^{-1}, respectively. On average, the differences between OMI-based and in situ seasonal relative trends are 1.6% yr^{-1}, -0.3% yr^{-1}, 1.0% yr^{-1}, and 1.4% yr^{-1} for the West, the Midwest, the Northeast, and the South regions, respectively. Note that the relative trends are calculated using coincident measurements for the comparisons. ~~The NO_2 relative trends from both datasets are expected to be close on a regional basis where surface emissions of NOx dominate the observed surface concentrations and tropospheric VCDs of NO_2.~~ The focus of this work is to ~~reconcile~~examine if the ~~difference~~differences between AQS in situ and OMI-based trends~~, which will be discussed in the following sections~~ can be reduced.

3.1.1 Improvement due to ocean trend correction

After removing the ocean trend as discussed in Section 2.3.1, the OMI-based NO_2 decreasing trends are more pronounced as shown in Fig. 4 ("Ocean", blue line) by 0.1-0.9% yr^{-1}. The regional relative trends have different sensitivities to the ocean trend removal due to different tropospheric VCDs levels. In general, the discrepancies between OMI-based and in situ trends are reduced except for the Midwest and the Northeast regions during DJF, which are already biased low. The averaged differences between OMI-based and in situ seasonal relative trends for the West, the Midwest, the Northeast, and the South regions are 1.2% yr^{-1}, -1.1% yr^{-1}, 0.4% yr^{-1}, and 1.0% yr^{-1}. Only in the Midwest region, removing the ocean trend enlarges the difference due to the large winter bias.

3.1.2 Improvement due to MODIS albedo update

The adoption of the up-to-date MODIS albedo (Section 2.3.2) greatly reduces the difference of relative trends in the Midwest during DJF from -3.6% yr^{-1} ("Ocean") to 1.3% yr^{-1} ("MODIS"), the improvement of DJF trend difference is more moderate from -1.7% to 0.5% (Fig. 4). There are no significant changes of the comparisons in other regions or other seasons. Fig. 5 shows the albedo seasonal relative trends for the 4 regions coincident with AQS in situ NO_2 data. The OMI DOMINO v2 incorporates a climatology albedo dataset (Kleipool et al., 2008) with snow/ice albedo adjustment ~~using~~, in which the albedo value is reset to be 0.6 if snow/ice is reported in the NASA Near-real-time Ice and Snow Extent (NISE) dataset (Boersma et al., 2011). The climatology albedo data ~~exhibits~~have no trends. Thus, the trends of albedo from the DOMINO v2 product mainly originate from the yearly variation of NISE detected snow/ice~~, followed by~~ and to a lesser extent the OMI sampling variation. The noticeable seasonal trend of the OMI DOMINO v2 albedo dataset is the 3.9% yr^{-1} increase in DJF of the Midwest and a smaller DJF increase (1.0%) of the Northeast. In contrast, the MODIS albedo dataset exhibits a smaller positive DJF trend (0.8% yr^{-1}), 3.1% yr^{-1} less than the trend from DOMINO v2, in the Midwest, and a small negative DJF trend (-0.8%) in the Northeast. These differences suggest that using a fixed snow/ice albedo and climatology albedo data are inadequate. The comparison to the AQS data shows that the MODIS albedo update leads to better agreement between satellite and in suit trends in winter in these regions (Fig. 4).

3.1.3 ~~Improvement due to~~Comparison after lightning event filter

As discussed in Section 2.3.3, lightning NOx affects the retrievals of satellite tropospheric NO_2 VCDs~~.~~ and NO_2 vertical mixing. Fig. 6 shows that the lightning filter significantly reduces the difference between the OMI-based relative trend and that of the AQS data by 0.5-1.4% yr^{-1} in the Northeast and 0.9-1.3% yr^{-1} in the South. As a result, the seasonal trend differences are within 0.9% yr^{-1} in these two regions except during SON. The Northeast is affected by the lightning filter due to lightning in this region and transport of lightning NOx from the South (Section 2.3.3). The lightning filter has little effect on the West and the Midwest. While lightning NOx can be significant during the monsoon season in some regions of the West (Fig. 3), the average tropospheric NO_2 VCDs are usually < $1x10^{15}$ molecules cm^{-2} and lightning affected regions are therefore excluded in trend analysis.

The effect of lightning filter (Fig. 6) cannot be shown in Fig. 4 because the coincident OMI and AQS data points are fewer after applying the lightning filter. We examine the improvements of ocean trend removal, MODIS albedo update, and data screening with the lightning filter by comparing the differences of different OMI-based seasonal relative trends from the AQS in situ trends in Fig. 7. The previously discussed improvements such as OMI albedo update for the Midwest and the Northeast during DJF are shown. By subtracting the AQS trends, we can now find clear improvements of the lightning filter for the South and the Northeast. There remains seasonal variation of OMI-based trend biases relative to in situ data but the discrepancies of the annual trends after the three discussed procedures are relatively small at 0.3% yr^{-1}, -0.3% yr^{-1}, -0.1% yr^{-1}, and 0.0% yr^{-1}, in the West, the Midwest, the Northeast, and the South regions (Fig. 1), respectively. The remaining seasonal difference of the

trends reflects in part the nonlinear photochemistry (Gu et al., 2013~~) and~~), the effects of NOx emission changes on NO_2 retrievals (Lamsal et al., 2015~~).~~), different spatial coverages of the two measurements, and the inherent difference between trends of NO_2 tropospheric VCDs and surface concentrations.

3.2 OMI-based NO_2 trends

Table 1 summarizes the regional annual trends of coincident AQS in situ and OMI data. The "Standard" OMI data (following the DOMINO v2 algorithm) tend to show less NO_2 reduction than AQS data. After applying the three ~~corrections~~data processing procedures discussed in the previous section to the OMI data, the agreement with the AQS trends is within the uncertainties of the trends. While lightning NOx is part of OMI NO_2 observations, we treat the influence of lightning on the OMI tropospheric VCD trend as a bias for comparison purposes in this study ~~since~~. Table 1 shows the effects of data sampling when both AQS and OMI data are ~~not as strongly affected by~~analyzed and when the lightning filter is applied.

Without the lightning filter, AQS decreasing trends are stronger than the decreasing trends of OMI data (Fig. 7). The lightning trend in the NLDN data is unclear due in part to the changing instrument sensitivity (Koshak et al., 2015). If lightning NOx is not accounted for in OMI retrieval, tropospheric NO_2 VCDs are overestimated. On the other hand, lightning accompanies low pressure systems which mix the atmosphere vertically and tend to reduce surface NO_2 concentrations when anthropogenic emissions are high such as urban and suburban regions. Therefore, lightning has opposite effects on surface and satellite trends. The low-pressure dilution effect on surface NO_2 concentrations depends on anthropogenic emissions (since the end point of dilution is the background NO_2 value). Therefore, the weaker decreasing surface trends likely reflects a reduction of low-pressure dilution effect. Similarly, as anthropogenic emissions decrease, the positive bias of tropospheric VCDs due to lightning NOx becomes larger, likely resulting in weaker decreasing trends. We consider the lightning effects on surface NO_2 trends to be mostly meteorological driven not by lightning NOx directly (e.g., Ott et al., 2010; Lu et al., 2017) and hence the filtered OMI NO_2 data are likely closer to emission related concentration changes.

The AQS in situ NO_2 annual relative trends (coincident with OMI data with lightning filter) are most significant in the Northeast (-5.2±0.6% yr^{-1}) and the West (-4.2±0.5% yr^{-1}), followed by the South (-3.0±0.5% yr^{-1}) and the Midwest (-2.8±0.6% yr^{-1}) regions. The nationwide annual trend is -4.1±0.4% yr^{-1}, which is consistent with the previous studies (Lamsal et al., 2015; Lu et al., 2015; Tong et al., 2015; de Foy et al., 2016b; Duncan et al., 2016; Krotkov et al., 2016). The significant NO_2 reductions result from updated technologies and strict regulations (Krotkov, et al., 2016). The ~~corrected~~ OMI-based NO_2 trends with the discussed procedures (coincident with AQS data) show similar reduction rates in the West (-3.8±0.4% yr^{-1}), the Midwest (-3.1±0.5% yr^{-1}), the Northeast (-5.3±0.7% yr^{-1}) and the South (-3.0±0.5% yr^{-1}) regions. The nationwide annual trend is -3.9±0.3% yr^{-1}.

One advantage of satellite observations over a surface monitoring network is spatial coverage. The processed OMI data ("Lightning filter") coincident with the AQS data show a national annual trend of -3.9±0.3% yr^{-1} similar to the AQS in situ trend of -4.1±0.4% yr^{-1}. Using all data available (Fig. 8, Table 1), the OMI data ("Lightning filter") show a much lower trend of -1.5±0.2%yr^{-1}, about half of the AQS trend (-3.9±0.4% yr^{-1}). Fig. 9 shows that the AQS sites, which are mostly urban and

suburban sites, tend to be located in regions with high tropospheric NO_2 VCDs. The OMI decreasing trend ~~with corrected data~~ is a function of tropospheric NO_2 VCDs, increasing from 0% yr^{-1} to -6% yr^{-1} (Fig. 9). The national annual trend is close to the value of clean regions which contribute much more than polluted regions. The larger decrease near the anthropogenic source regions reflect in part the nonlinear photochemistry (Gu et al., 2013) and in part to a stronger influence of NOx sources such as soils in rural regions.

4. Conclusions

Using data from the DOMINO v2 algorithm, we find that the computed OMI-based seasonal NO_2 (relative) trends underestimate the decreasing trends of the EPA AQS data by up to 3.7% yr^{-1}. ~~We attribute most of the discrepancies to OMI retrievals since the standard retrieval algorithm was not specifically designed for trend analysis.~~ While lightning NOx is part of OMI NO_2 observations, we treat the influence of lightning on the OMI tropospheric VCD trend as a bias for comparison purposes in this study ~~since AQS data are not as strongly affected by lightning.~~. Furthermore, lightning NOx effects need to be removed when using satellite observations to understand the effects of changing anthropogenic emissions.

In this study, we show that removing the background ocean trend ~~(likely a result of the increasing stripes),~~ adopting MODIS albedo data (with better temporospatial resolutions and characterization of snow/ice), and excluding lightning influences can bring OMI tropospheric NO_2 VCD trends in close agreement (within 0.3% yr^{-1}) with those of the AQS data. Among the corrections, the background ocean trend removal is not as significant as the latter two. Since the origin of this trend is not yet clear, the ocean trend removal method may need updates in future studies. The remaining differences may result from the inherent differences between trends of NO_2 tropospheric VCDs and surface concentrations, different spatial sampling of the measurements, chemical-nonlinearity, and tropospheric NO_2 profile changes. The largest effects of MODIS albedo update are in winter in Midwest and Northeast and those of lightning filter are in the South and the Northeast. After applying these ~~corrections~~data processing procedures, the derived OMI-based annual regional NO_2 trends change by a factor of > 2 for the South, the Midwest, and the West and seasonal changes can be even larger. We derive ~~optimized~~ OMI-based NO_2 regional annual relative trends using all available data for the West (-2.0%±0.3 yr^{-1}), the Midwest (-1.8%±0.4 yr^{-1}), the Northeast (-3.1%±0.5 yr^{-1}), and the South (-0.9%±0.3 yr^{-1}).

The national annual trend of the ~~corrected~~processed OMI data is -1.5±0.2%yr^{-1}, about half of the AQS trend (-3.9±0.4% yr^{-1}). It reflects that the AQS sites are mostly located in the urban and suburban regions, where OMI data show much larger decreasing trends (up to -6% yr^{-1}) than rural regions (down to 0% yr^{-1}). The reasons for the dependence of OMI derived trends on tropospheric NO_2 VCDs and the seasonal/regional trend differences are still not completely understood. Further studies are necessary to improve our understanding of these trends. The observation-based lightning filter implemented in this study is preliminary. Incorporating chemical transport modeling may improve this filter. Moreover, the results presented here represent an alternative and indirect way to assess the importance of lightning NOx for National Climate Assessment (NCA) analyses

described in Koshak et al. (2015), and Koshak (2017). Inversion studies (e.g., Zhao and Wang, 2009; Gu et al., 2013, 2014, 2016) will be needed to quantify the emission and AMF changes corresponding to the OMI tropospheric NO_2 VCD trends.

Acknowledgements

This work was supported by the NASA ACMAP Program and the NASA Climate Indicators and Data Products for Future National Climate Assessments (NNH14ZDA001N-INCA). We thank data sources, including DOMINO v2 OMI data from KNMI, MODIS data from NASA, and EPA AQS NO_2 data from EPA. In addition, the authors gratefully acknowledge Vaisala Inc. for providing the NLDN data used in this study. K. Folkert Boersma acknowledges funding from the EU FP7 project QA4ECV (grant no. 607405).

Data access

The datasets used in this research have been obtained online as follows:

- DOMINO v2 NO_2 retrievals: http://www.temis.nl/airpollution/no2.html
- EPA AQS NO_2 data: US Environmental Protection Agency. Air Quality System Data Mart [internet database] available at http://www.epa.gov/ttn/airs/aqsdatamart.
- NLDN lightning data: https://lightning.nsstc.nasa.gov/data/data_nldn.html
- MODIS MCD43B3 data: https://lpdaac.usgs.gov/dataset_discovery/modis/modis_products_table/mcd43b3

References

Bey, I., Jacob, D. J., Yantosca, R. M., Logan, J. A., Field, B. D., Fiore, A. M., Li, Q. B., Liu, H. G. Y., Mickley, L. J., and Schultz, M. G.: Global modeling of tropospheric chemistry with assimilated meteorology: Model description and evaluation, J. Geophys. Res.-Atmos., 106, 23073-23095, 10.1029/2001jd000807, 2001.

Boersma, K. F., Eskes, H. J., and Brinksma, E. J.: Error analysis for tropospheric NO_2 retrieval from space, J. Geophys. Res.-Atmos., 109, 10.1029/2003JD003962, 2004.

Boersma, K. F., Eskes, H. J., Veefkind, J. P., Brinksma, E. J., van der A, R. J., Sneep, M., van den Oord, G. H. J., Levelt, P. F., Stammes, P., Gleason, J. F., and Bucsela, E. J.: Near-real time retrieval of tropospheric NO_2 from OMI, Atmos. Chem. Phys., 7, 2103-2118, 10.5194/acp-7-2103-2007, 2007.

Boersma, K. F., Eskes, H. J., Dirksen, R. J., van der A, R. J., Veefkind, J. P., Stammes, P., Huijnen, V., Kleipool, Q. L., Sneep, M., Claas, J., Leitão, J., Richter, A., Zhou, Y., and Brunner, D.: An improved tropospheric NO_2 column retrieval algorithm for the Ozone Monitoring Instrument, Atmos. Meas. Tech., 4, 1905-1928, 10.5194/amt-4-1905-2011, 2011.

Bucsela, E. J., Pickering, K. E., Huntemann, T. L., Cohen, R. C., Perring, A., Gleason, J. F., Blakeslee, R. J., Albrecht, R. I., Holzworth, R., Cipriani, J. P., Vargas-Navarro, D., Mora-Segura, I., Pacheco-Hernández, A., and Laporte-Molina, S.:

Lightning-generated NOx seen by the Ozone Monitoring Instrument during NASA's Tropical Composition, Cloud and Climate Coupling Experiment (TC4), J. Geophys. Res.-Atmos., 115, 10.1029/2009JD013118, 2010.

Castellanos, P., and Boersma, K. F.: Reductions in nitrogen oxides over Europe driven by environmental policy and economic recession, Sci. Rep., 2, 265, 10.1038/srep00265, 2012.

Choi, Y., Wang, Y., Zeng, T., Martin, R. V., Kurosu, T. P., and Chance, K.: Evidence of lightning NOx and convective transport of pollutants in satellite observations over North America, Geophys. Res. Lett., 32, L02805, 10.1029/2004GL021436, 2005.

Choi, Y., Wang, Y., Zeng, T., Cunnold, D., Yang, E.-S., Martin, R., Chance, K., Thouret, V., and Edgerton, E.: Springtime transitions of NO_2, CO, and O_3 over North America: Model evaluation and analysis, J. Geophys. Res.-Atmos., 113, D20311, 10.1029/2007JD009632, 2008a.

Choi, Y., Wang, Y., Yang, Q., Cunnold, D., Zeng, T., Shim, C., Luo, M., Eldering, A., Bucsela, E., and Gleason, J.: Spring to summer northward migration of high O_3 over the western North Atlantic, Geophys. Res. Lett., 35, L04818, 10.1029/2007GL032276, 2008b.

Cui, Y., Lin, J., Song, C., Liu, M., Yan, Y., Xu, Y., and Huang, B.: Rapid growth in nitrogen dioxide pollution over Western China, 2005–2013, Atmos. Chem. Phys., 16, 6207-6221, 10.5194/acp-16-6207-2016, 2016.

Cummins, K. L., and Murphy, M. J.: An Overview of Lightning Locating Systems: History, Techniques, and Data Uses, With an In-Depth Look at the U.S. NLDN, IEEE Transactions on Electromagnetic Compatibility, 51, 499-518, 10.1109/TEMC.2009.2023450, 2009.

de Foy, B., Lu, Z., and Streets, D. G.: Satellite NO_2 retrievals suggest China has exceeded its NOx reduction goals from the twelfth Five-Year Plan, Sci. Rep., 6, 35912, 10.1038/srep35912, 2016a.

de Foy, B., Lu, Z., and Streets, D. G.: Impacts of control strategies, the Great Recession and weekday variations on NO_2 columns above North American cities, Atmos. Environ., 138, 74-86, j.atmosenv.2016.04.038, 2016b.

Demerjian, K. L.: A review of national monitoring networks in North America, Atmos. Environ., 34, 1861-1884, 10.1016/S1352-2310(99)00452-5, 2000.

Dirksen, R. J., Boersma, K. F., Eskes, H. J., Ionov, D. V., Bucsela, E. J., Levelt, P. F., and Kelder, H. M.: Evaluation of stratospheric NO2 retrieved from the Ozone Monitoring Instrument: Intercomparison, diurnal cycle, and trending, J. Geophys. Res.-Atmos., 116, 10.1029/2010JD014943, 2011.

Duncan, B. N., Yoshida, Y., de Foy, B., Lamsal, L. N., Streets, D. G., Lu, Z. F., Pickering, K. E., and Krotkov, N. A.: The observed response of Ozone Monitoring Instrument (OMI) NO2 columns to NOx emission controls on power plants in the United States: 2005-2011, Atmospheric Environment, 81, 102-111, 10.1016/j.atmosenv.2013.08.068, 2013.

Duncan, B. N., Lamsal, L. N., Thompson, A. M., Yoshida, Y., Lu, Z., Streets, D. G., Hurwitz, M. M., and Pickering, K. E.: A space-based, high-resolution view of notable changes in urban NOx pollution around the world (2005–2014), J. Geophys. Res.-Atmos., 121, 976-996, 10.1002/2015JD024121, 2016.

Eskes, H. J., and Boersma, K. F.: Averaging kernels for DOAS total-column satellite retrievals, Atmos. Chem. Phys., 3, 1285-1291, 10.5194/acp-3-1285-2003, 2003.

Gu, D. S., Wang, Y. H., Smeltzer, C., and Liu, Z.: Reduction in NOx Emission Trends over China: Regional and Seasonal Variations, Environ. Sci. Technol., 47, 12912-12919, 10.1021/es401727e, 2013.

Gu, D., Wang, Y., Smeltzer, C., and Boersma, K. F.: Anthropogenic emissions of NOx over China: Reconciling the difference of inverse modeling results using GOME-2 and OMI measurements, J. Geophys. Res.-Atmos., 119, 2014JD021644, 10.1002/2014JD021644, 2014.

Gu, D., Wang, Y., Yin, R., Zhang, Y., and Smeltzer, C.: Inverse modelling of NOx emissions over eastern China: uncertainties due to chemical non-linearity, Atmos. Meas. Tech., 9, 5193-5201, 10.5194/amt-9-5193-2016, 2016.

Guenther, A. B., Jiang, X., Heald, C. L., Sakulyanontvittaya, T., Duhl, T., Emmons, L. K., and Wang, X.: The Model of Emissions of Gases and Aerosols from Nature version 2.1 (MEGAN2.1): an extended and updated framework for modeling biogenic emissions, Geosci. Model Dev., 5, 1471-1492, 10.5194/gmd-5-1471-2012, 2012.

Heckel, A., Kim, S. W., Frost, G. J., Richter, A., Trainer, M., and Burrows, J. P.: Influence of low spatial resolution a priori data on tropospheric NO_2 satellite retrievals, Atmos. Meas. Tech., 4, 1805-1820, 10.5194/amt-4-1805-2011, 2011.

Jiakui, T., Aijun, Z., and Zhengmin, H.: The earth surface reflectance retrieval by exploiting the synergy of TERRA and AQUA MODIS data, 2007 IEEE International Geoscience and Remote Sensing Symposium, 2007, 1697-1700,

Kain, J. S., and Fritsch, J. M.: Convective Parameterization for Mesoscale Models: The Kain-Fritsch Scheme, in: The Representation of Cumulus Convection in Numerical Models, edited by: Emanuel, K. A., and Raymond, D. J., Am. Meteorol. Soc., Boston, MA, 165-170, 1993.

Kendall, M. G.: Rank correlation methods, Rank correlation methods., Griffin, Oxford, England, 1948.

Kleipool, Q. L., Dobber, M. R., de Haan, J. F., and Levelt, P. F.: Earth surface reflectance climatology from 3 years of OMI data, J. Geophys. Res.-Atmos., 113, 10.1029/2008JD010290, 2008.

Koshak, W., Peterson, H., Biazar, A., Khan, M., and Wang, L.: The NASA Lightning Nitrogen Oxides Model (LNOM): Application to air quality modeling, Atmos. Res., 135–136, 363-369, 10.1016/j.atmosres.2012.12.015, 2014.

Koshak, W. J., Cummins, K. L., Buechler, D. E., Vant-Hull, B., Blakeslee, R. J., Williams, E. R., and Peterson, H. S.: Variability of CONUS Lightning in 2003–12 and Associated Impacts, J. Appl. Meteorol. Clim., 54, 15-41, 10.1175/jamc-d-14-0072.1, 2015.

Koshak, W. J., Lightning NOx estimates from space-based lightning imagers, 16th Annual Community Modeling and Analysis System (CMAS) Conference, Chapel Hill, NC, October 23-25, 2017.

Krotkov, N., Herman, J., Bhartia, P. K., Seftor, C., Arola, A., Kaurola, J., Koskinen, L., Kalliskota, S., Taalas, P., and Geogdzhaev, I.: Version 2 TOMS UV algorithm: problems and enhancements, in: P Soc Photo-Opt Ins, edited by: Slusser, J. R., Herman, J. R., and Gao, W., Proceedings of the Society of Photo-Optical Instrumentation Engineers (Spie), Spie-Int Soc Optical Engineering, Bellingham, 82-93, 2002.

Krotkov, N. A., McLinden, C. A., Li, C., Lamsal, L. N., Celarier, E. A., Marchenko, S. V., Swartz, W. H., Bucsela, E. J., Joiner, J., Duncan, B. N., Boersma, K. F., Veefkind, J. P., Levelt, P. F., Fioletov, V. E., Dickerson, R. R., He, H., Lu, Z., and Streets, D. G.: Aura OMI observations of regional SO_2 and NO_2 pollution changes from 2005 to 2015, Atmos. Chem. Phys., 16, 4605-4629, 10.5194/acp-16-4605-2016, 2016.

Lamsal, L. N., Martin, R. V., van Donkelaar, A., Steinbacher, M., Celarier, E. A., Bucsela, E., Dunlea, E. J., and Pinto, J. P.: Ground-level nitrogen dioxide concentrations inferred from the satellite-borne Ozone Monitoring Instrument, J. Geophys. Res.-Atmos., 113, 10.1029/2007JD009235, 2008.

Lamsal, L. N., Martin, R. V., van Donkelaar, A., Celarier, E. A., Bucsela, E. J., Boersma, K. F., Dirksen, R., Luo, C., and Wang, Y.: Indirect validation of tropospheric nitrogen dioxide retrieved from the OMI satellite instrument: Insight into the seasonal variation of nitrogen oxides at northern midlatitudes, J. Geophys. Res.-Atmos., 115, 10.1029/2009JD013351, 2010.

Lamsal, L. N., Krotkov, N. A., Celarier, E. A., Swartz, W. H., Pickering, K. E., Bucsela, E. J., Gleason, J. F., Martin, R. V., Philip, S., Irie, H., Cede, A., Herman, J., Weinheimer, A., Szykman, J. J., and Knepp, T. N.: Evaluation of OMI operational standard NO2 column retrievals using in situ and surface-based NO2 observations, Atmos. Chem. Phys., 14, 11587-11609, 10.5194/acp-14-11587-2014, 2014.

Lamsal, L. N., Duncan, B. N., Yoshida, Y., Krotkov, N. A., Pickering, K. E., Streets, D. G., and Lu, Z.: U.S. NO2 trends (2005–2013): EPA Air Quality System (AQS) data versus improved observations from the Ozone Monitoring Instrument (OMI), Atmos. Environ., 110, 130-143, j.atmosenv.2015.03.055, 2015.

Laughner, J. L., Zare, A., and Cohen, R. C.: Effects of daily meteorology on the interpretation of space-based remote sensing of NO_2, Atmos. Chem. Phys., 16, 15247-15264, 10.5194/acp-16-15247-2016, 2016.

Lin, J. T., McElroy, M. B., and Boersma, K. F.: Constraint of anthropogenic NOx emissions in China from different sectors: a new methodology using multiple satellite retrievals, Atmos. Chem. Phys., 10, 63-78, 10.5194/acp-10-63-2010, 2010.

Lin, J. T., and McElroy, M. B.: Detection from space of a reduction in anthropogenic emissions of nitrogen oxides during the Chinese economic downturn, Atmos. Chem. Phys., 11, 8171-8188, 10.5194/acp-11-8171-2011, 2011.

Lin, J. T., Liu, Z., Zhang, Q., Liu, H., Mao, J., and Zhuang, G.: Modeling uncertainties for tropospheric nitrogen dioxide columns affecting satellite-based inverse modeling of nitrogen oxides emissions, Atmos. Chem. Phys., 12, 12255-12275, 10.5194/acp-12-12255-2012, 2012.

Lin, J. T., Pan, D., and Zhang, R.: Trend and Interannual Variability of Chinese Air Pollution since 2000 in Association with Socioeconomic Development: A Brief Overview, Atmos. Oceanic Sci. Lett., 6, 84-89, 10.1080/16742834.2013.11447061, 2013.

Lin, J. T., Martin, R. V., Boersma, K. F., Sneep, M., Stammes, P., Spurr, R., Wang, P., Van Roozendael, M., Clémer, K., and Irie, H.: Retrieving tropospheric nitrogen dioxide from the Ozone Monitoring Instrument: effects of aerosols, surface reflectance anisotropy, and vertical profile of nitrogen dioxide, Atmos. Chem. Phys., 14, 1441-1461, 10.5194/acp-14-1441-2014, 2014.

Lin, J. T., Liu, M. Y., Xin, J. Y., Boersma, K. F., Spurr, R., Martin, R., and Zhang, Q.: Influence of aerosols and surface reflectance on satellite NO_2 retrieval: seasonal and spatial characteristics and implications for NOx emission constraints, Atmos. Chem. Phys., 15, 11217-11241, 10.5194/acp-15-11217-2015, 2015.

Liu, F., Beirle, S., Zhang, Q., van der A, R. J., Zheng, B., Tong, D., and He, K.: NOx emission trends over Chinese cities estimated from OMI observations during 2005 to 2015, Atmos. Chem. Phys., 17, 9261-9275, 10.5194/acp-17-9261-2017, 2017.

Liu, Z., Wang, Y., Gu, D., Zhao, C., Huey, L. G., Stickel, R., Liao, J., Shao, M., Zhu, T., Zeng, L., Liu, S.-C., Chang, C.-C., Amoroso, A., and Costabile, F.: Evidence of Reactive Aromatics As a Major Source of Peroxy Acetyl Nitrate over China, Environ. Sci. Technol., 44, 7017-7022, 10.1021/es1007966, 2010.

Liu, Z., Wang, Y., Vrekoussis, M., Richter, A., Wittrock, F., Burrows, J. P., Shao, M., Chang, C.-C., Liu, S.-C., Wang, H., and Chen, C.: Exploring the missing source of glyoxal (CHOCHO) over China, Geophys. Res. Lett., 39, L10812, 10.1029/2012GL051645, 2012a.

Liu, Z., Wang, Y., Gu, D., Zhao, C., Huey, L. G., Stickel, R., Liao, J., Shao, M., Zhu, T., Zeng, L., Amoroso, A., Costabile, F., Chang, C. C., and Liu, S. C.: Summertime photochemistry during CAREBeijing-2007: ROx budgets and O3 formation, Atmos. Chem. Phys., 12, 7737-7752, 10.5194/acp-12-7737-2012, 2012b.

Lorente, A., Folkert Boersma, K., Yu, H., Dörner, S., Hilboll, A., Richter, A., Liu, M., Lamsal, L. N., Barkley, M., De Smedt, I., Van Roozendael, M., Wang, Y., Wagner, T., Beirle, S., Lin, J. T., Krotkov, N., Stammes, P., Wang, P., Eskes, H. J., and Krol, M.: Structural uncertainty in air mass factor calculation for NO2 and HCHO satellite retrievals, Atmos. Meas. Tech., 10, 759-782, 10.5194/amt-10-759-2017, 2017.

Lu, Z., Streets, D. G., de Foy, B., Lamsal, L. N., Duncan, B. N., and Xing, J.: Emissions of nitrogen oxides from US urban areas: estimation from Ozone Monitoring Instrument retrievals for 2005–2014, Atmos. Chem. Phys., 15, 10367-10383, 10.5194/acp-15-10367-2015, 2015.

Luo, C., Wang, Y., and Koshak, W. J.: Development of a self-consistent lightning NOx simulation in large-scale 3-D models, J. Geophys. Res.-Atmos., 122, 3141-3154, 10.1002/2016JD026225, 2017.

Mann, H. B.: NONPARAMETRIC TESTS AGAINST TREND, Econometrica, 13, 245-259, 10.2307/1907187, 1945.

Martin, R. V., Sauvage, B., Folkins, I., Sioris, C. E., Boone, C., Bernath, P., and Ziemke, J.: Space-based constraints on the production of nitric oxide by lightning, J. Geophys. Res.-Atmos., 112, 10.1029/2006JD007831, 2007.

Ott, L. E., Pickering, K. E., Stenchikov, G. L., Allen, D. J., DeCaria, A. J., Ridley, B., Lin, R.-F., Lang, S., and Tao, W.-K.: Production of lightning NOx and its vertical distribution calculated from three-dimensional cloud-scale chemical transport model simulations, J. Geophys. Res.-Atmos., 115, 10.1029/2009JD011880, 2010.

Pickering, K. E., Wang, Y., Tao, W.-K., Price, C., and Müller, J.-F.: Vertical distributions of lightning NOx for use in regional and global chemical transport models, J. Geophys. Res.-Atmos., 103, 31203-31216, 10.1029/98JD02651, 1998.

Rudlosky, S. D., and Fuelberg, H. E.: Pre- and Postupgrade Distributions of NLDN Reported Cloud-to-Ground Lightning Characteristics in the Contiguous United States, Mon. Weather Rev., 138, 3623-3633, 10.1175/2010mwr3283.1, 2010.

Russell, A. R., Perring, A. E., Valin, L. C., Bucsela, E. J., Browne, E. C., Wooldridge, P. J., and Cohen, R. C.: A high spatial resolution retrieval of NO_2 column densities from OMI: method and evaluation, Atmos. Chem. Phys., 11, 8543-8554, 10.5194/acp-11-8543-2011, 2011.

Russell, A. R., Valin, L. C., and Cohen, R. C.: Trends in OMI NO_2 observations over the United States: effects of emission control technology and the economic recession, Atmos. Chem. Phys., 12, 12197-12209, 10.5194/acp-12-12197-2012, 2012.

Saha, S., Moorthi, S., Pan, H.-L., Wu, X., Wang, J., Nadiga, S., Tripp, P., Kistler, R., Woollen, J., Behringer, D., Liu, H., Stokes, D., Grumbine, R., Gayno, G., Wang, J., Hou, Y.-T., Chuang, H.-Y., Juang, H.-M. H., Sela, J., Iredell, M., Treadon, R., Kleist, D., Van Delst, P., Keyser, D., Derber, J., Ek, M., Meng, J., Wei, H., Yang, R., Lord, S., Van Den Dool, H., Kumar, A., Wang, W., Long, C., Chelliah, M., Xue, Y., Huang, B., Schemm, J.-K., Ebisuzaki, W., Lin, R., Xie, P., Chen, M., Zhou, S., Higgins, W., Zou, C.-Z., Liu, Q., Chen, Y., Han, Y., Cucurull, L., Reynolds, R. W., Rutledge, G., and Goldberg, M.: The NCEP Climate Forecast System Reanalysis, Bulletin of the Am. Meteorol. Soc., 91, 1015-1057, 10.1175/2010BAMS3001.1, 2010.

Schaaf, C. B., Gao, F., Strahler, A. H., Lucht, W., Li, X., Tsang, T., Strugnell, N. C., Zhang, X., Jin, Y., Muller, J.-P., Lewis, P., Barnsley, M., Hobson, P., Disney, M., Roberts, G., Dunderdale, M., Doll, C., d'Entremont, R. P., Hu, B., Liang, S., Privette, J. L., and Roy, D.: First operational BRDF, albedo nadir reflectance products from MODIS, Remote Sens. Environ., 83, 135-148, 10.1016/S0034-4257(02)00091-3, 2002.

Schenkeveld, V. M. E., Jaross, G., Marchenko, S., Haffner, D., Kleipool, Q. L., Rozemeijer, N. C., Veefkind, J. P., and Levelt, P. F.: In-flight performance of the Ozone Monitoring Instrument, Atmos. Meas. Tech., 10, 1957-1986, 10.5194/amt-10-1957-2017, 2017.

Tang, J. K., and Zhang, A. J.: The earth surface reflectance retrieval by exploiting the synergy of TERRA and AQUA MODIS data, Int. Geosci. Remote Se., 1697-1700, 10.1109/Igarss.2007.4423144, 2007.

Tong, D. Q., Lamsal, L., Pan, L., Ding, C., Kim, H., Lee, P., Chai, T., Pickering, K. E., and Stajner, I.: Long-term NOx trends over large cities in the United States during the great recession: Comparison of satellite retrievals, ground observations, and emission inventories, Atmos. Environ., 107, 70-84, 10.1016/j.atmosenv.2015.01.035, 2015.

Yang, Q., Wang, Y., Zhao, C., Liu, Z., Gustafson, W. I., and Shao, M.: NOx Emission Reduction and its Effects on Ozone during the 2008 Olympic Games, Environ. Sci. Technol., 45, 6404-6410, 10.1021/es200675v, 2011.

Zara, M., Boersma, K. F., De Smedt, I., Richter, A., Peters, E., Van Geffen, J. H. G. M., Beirle, S., Wagner, T., Van Roozendael, M., Marchenko, S., Lamsal, L. N., and Eskes, H. J.: Improved slant column density retrieval of nitrogen dioxide and formaldehyde for OMI and GOME-2A from QA4ECV: intercomparison, uncertainty characterization, and trends, Atmos. Meas. Tech. Discuss., 2018, 1-47, 10.5194/amt-2017-453, 2018.

Zhang, R., Wang, Y., He, Q., Chen, L., Zhang, Y., Qu, H., Smeltzer, C., Li, J., Alvarado, L. M. A., Vrekoussis, M., Richter, A., Wittrock, F., and Burrows, J. P.: Enhanced trans-Himalaya pollution transport to the Tibetan Plateau by cut-off low systems, Atmos. Chem. Phys., 17, 3083-3095, 10.5194/acp-17-3083-2017, 2017.

Zhang, Y., Wang, Y., Chen, G., Smeltzer, C., Crawford, J., Olson, J., Szykman, J., Weinheimer, A. J., Knapp, D. J., Montzka, D. D., Wisthaler, A., Mikoviny, T., Fried, A., and Diskin, G.: Large vertical gradient of reactive nitrogen oxides in the boundary layer: Modeling analysis of DISCOVER-AQ 2011 observations, J. Geophys. Res.-Atmos., 121, 1922-1934, 10.1002/2015JD024203, 2016a.

Zhang, Y., and Wang, Y.: Climate-driven ground-level ozone extreme in the fall over the Southeast United States, P. Natl. Acad. Sci., 113, 10025-10030, 10.1073/pnas.1602563113, 2016b.

Zhao, C., Wang, Y., Choi, Y., and Zeng, T.: Summertime impact of convective transport and lightning NOx production over North America: modeling dependence on meteorological simulations, Atmos. Chem. Phys., 9, 4315-4327, 10.5194/acp-9-4315-2009, 2009a.

Zhao, C., and Wang, Y.: Assimilated inversion of NOx emissions over east Asia using OMI NO_2 column measurements, Geophys. Res. Lett., 36, L06805, 10.1029/2008GL037123, 2009b.

Zhou, Y., Brunner, D., Boersma, K. F., Dirksen, R., and Wang, P.: An improved tropospheric NO_2 retrieval for OMI observations in the vicinity of mountainous terrain, Atmos. Meas. Tech., 2, 401-416, 10.5194/amt-2-401-2009, 2009.

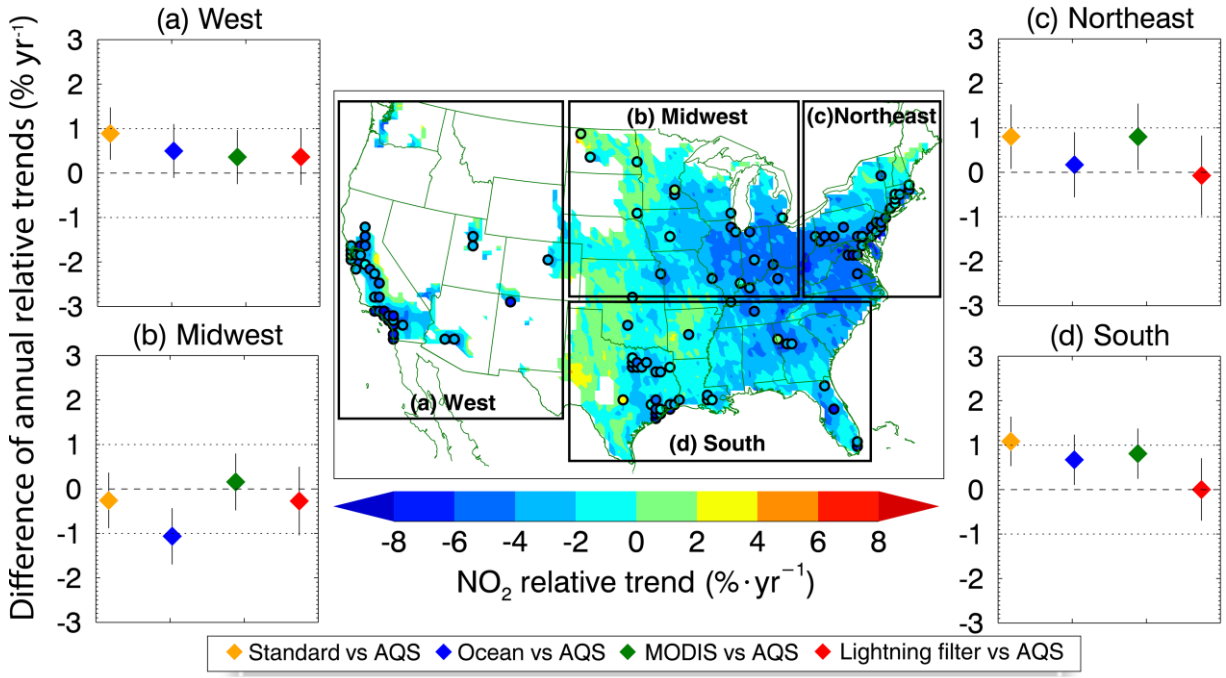

Figure 1. The solid black borders in the center map define the four regions used in this study. The colored background shows the OMI-based NO_2 annual relative trends of the "~~lightning~~Lightning filter" data. Grid cells with 2005-2014 mean NO_2 VCD values < $1x10^{15}$ molecules cm^{-2} are excluded in this study and are shown in white. The black bordered circles represent the locations of AQS sites. Panel (a) through (d) show the regional difference (OMI-based relative trends minus AQS relative trends) of annual relative trends between coincident OMI-based and AQS in situ data. The colored diamonds are for "Standard" (orange), "Ocean" (blue), "MODIS" (green), and "Lightning filter" (red) OMI data, respectively. The different OMI VCD data are described in Section 2.4.

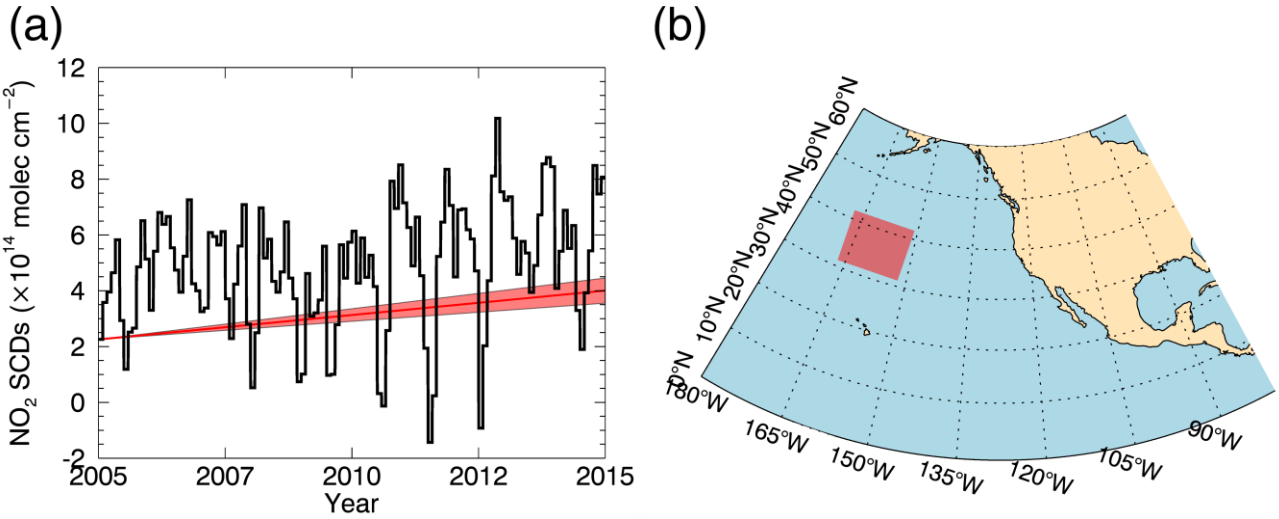

Figure 2. The black line in panel (a) shows the monthly averaged OMI tropospheric NO_2 VCD values in the North Pacific region (red box in panel (b)) from 2005 to 2014. The red line in panel (a) represents the ocean trend used in this research, with the 95th percentile confidence intervals shaded in red.

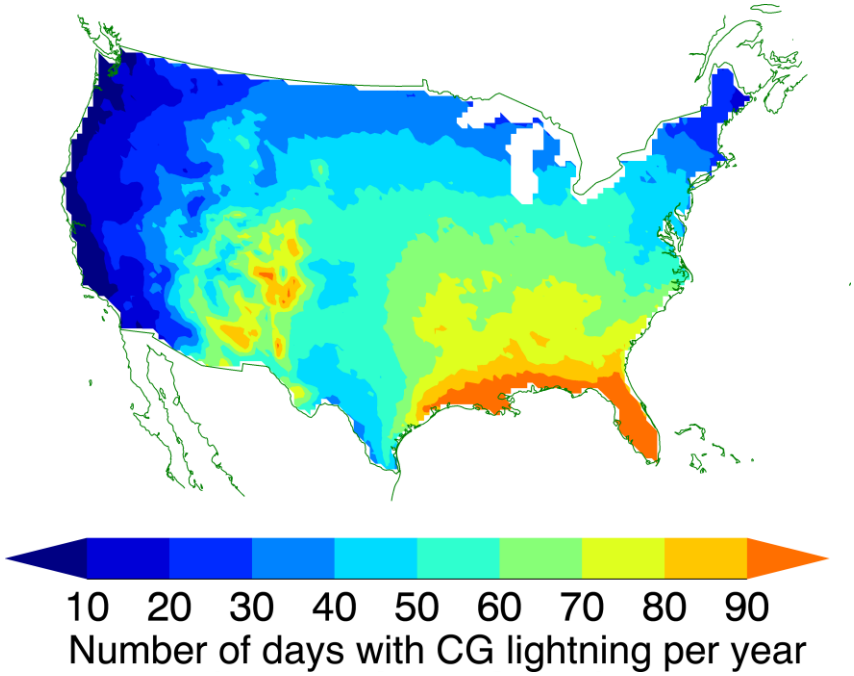

Figure 3. Number of days with NLDN detected cloud-to-ground (CG) lightning per model grid cell per year during 2005-2014. The lightning occurrences are calculated using the REAM grid resolution.

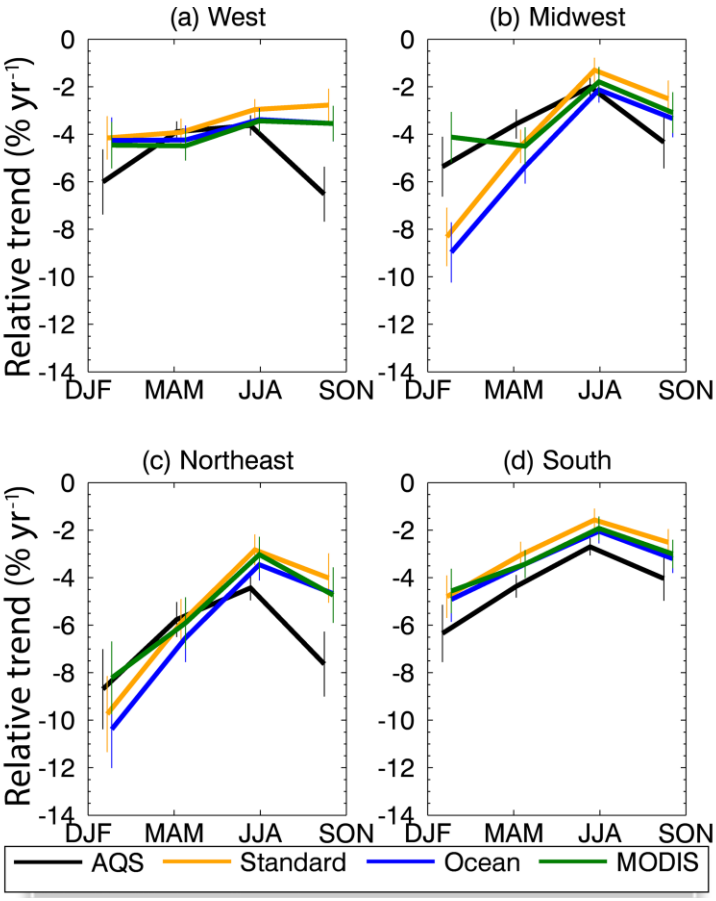

Figure 4. Seasonal relative trends of NO_2 calculated from the AQS in situ measurements ("AQS", black line) and those derived from different OMI VCD data ("Standard", orange line; "Ocean", blue line; "MODIS", green line). The error bars represent 95th percentile confidence intervals.

5

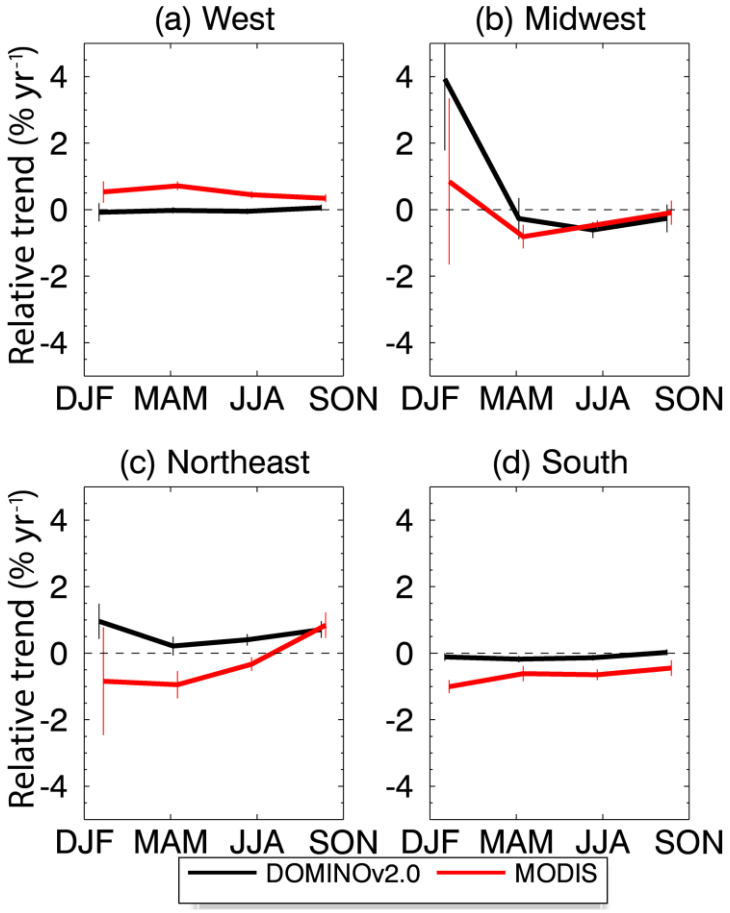

Figure 5. Seasonal relative albedo trends of OMI (black line) and MODIS (red line) surface reflectance products, coincident with AQS in situ data used in Figure 5. The error bars represent 95th percentile confidence intervals.

5

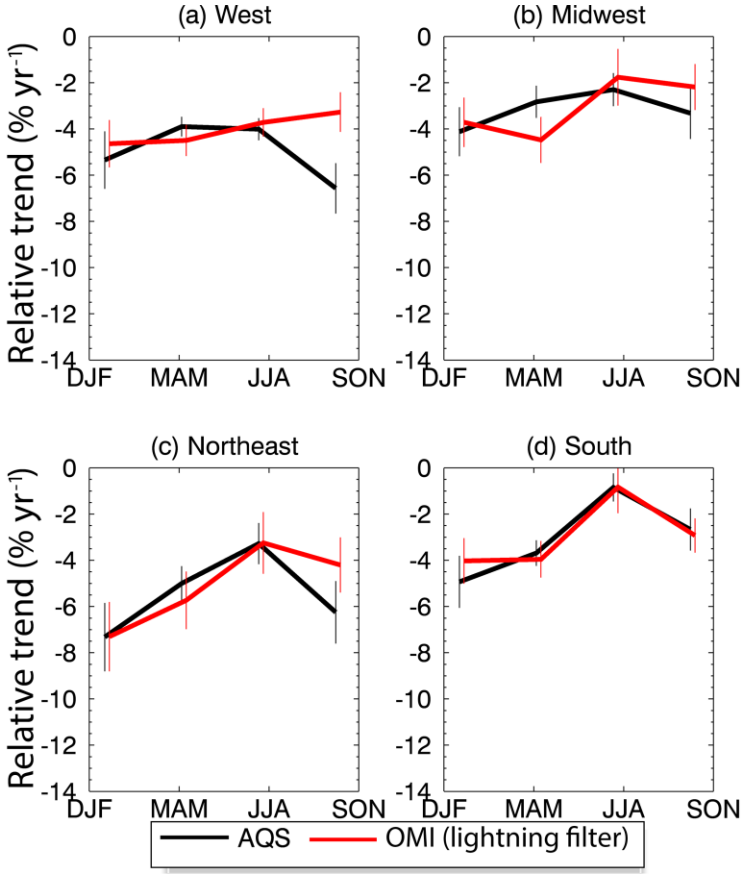

Figure 6. Seasonal relative trends of NO_2 calculated from the AQS in situ measurements ("AQS", black line) and those derived from OMI data after applying the lightning filter ("OMI (lightning filter)", red line). The error bars represent 95th percentile confidence intervals. The coincident data points are less than those used in Figure 5 and therefore the AQS trends are not the same.

5

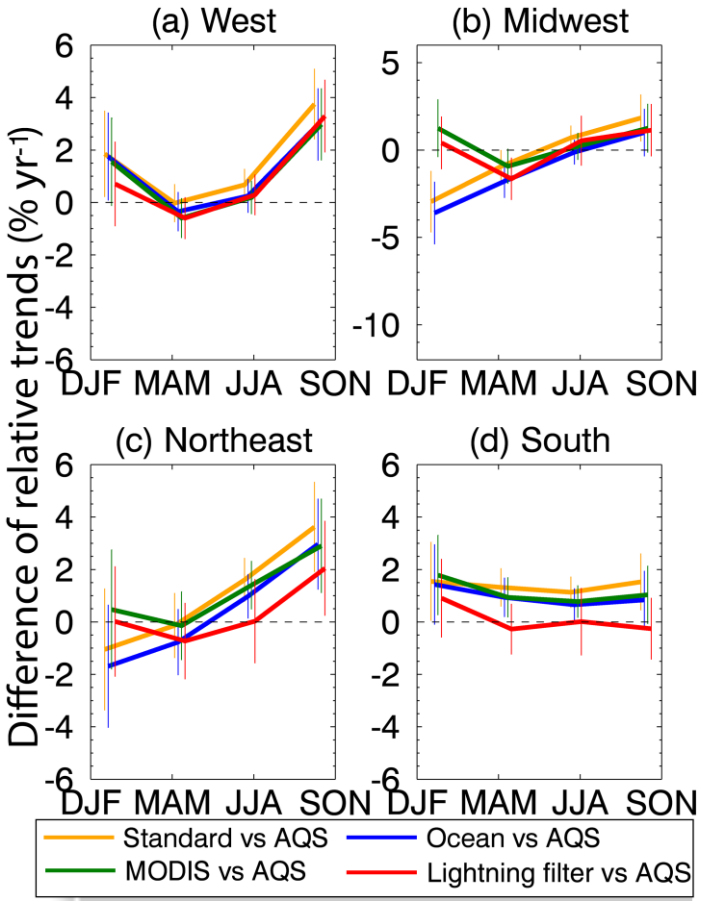

Figure 7. Seasonal differences of OMI-based relative trends from those computed from AQS in situ data. The error bars represent 95th percentile confidence intervals. The relative trends are shown in Figs. 4 and 6. The figure legends are the same as in Figs. 4 and 6 but with the AQS trends subtracted from the OMI-based trends.

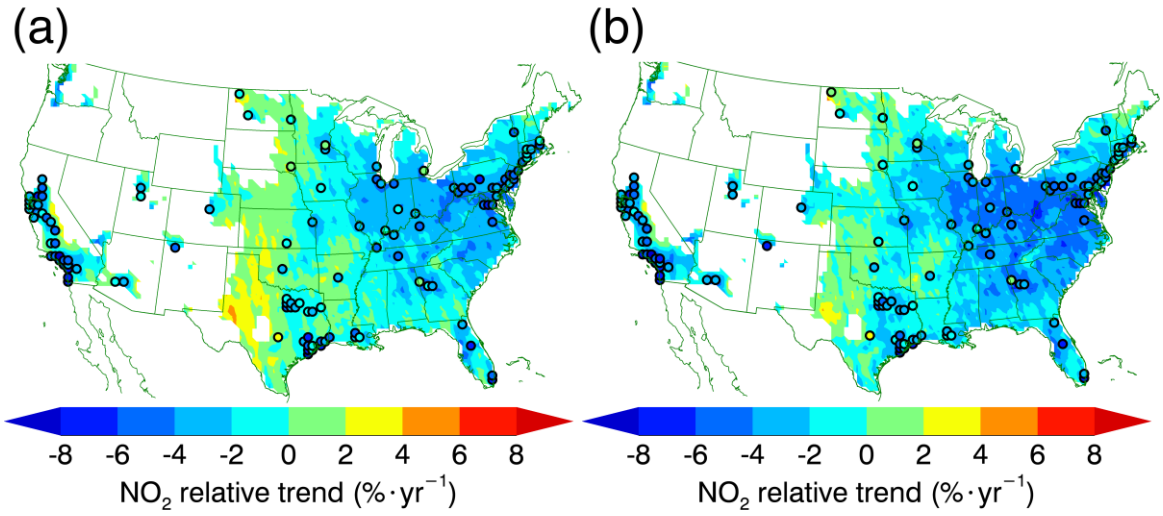

Figure 8: Annual relative trends of OMI-based NO_2 for "Standard" (a) and for "Lightning filter" (b) as the colored background. Black bordered circles indicate corresponding AQS NO_2 trends. Grid cells with 2005-2014 mean NO_2 VCDs < $1x10^{15}$ molecules cm^{-2} are excluded in the analysis and are shown in white.

5

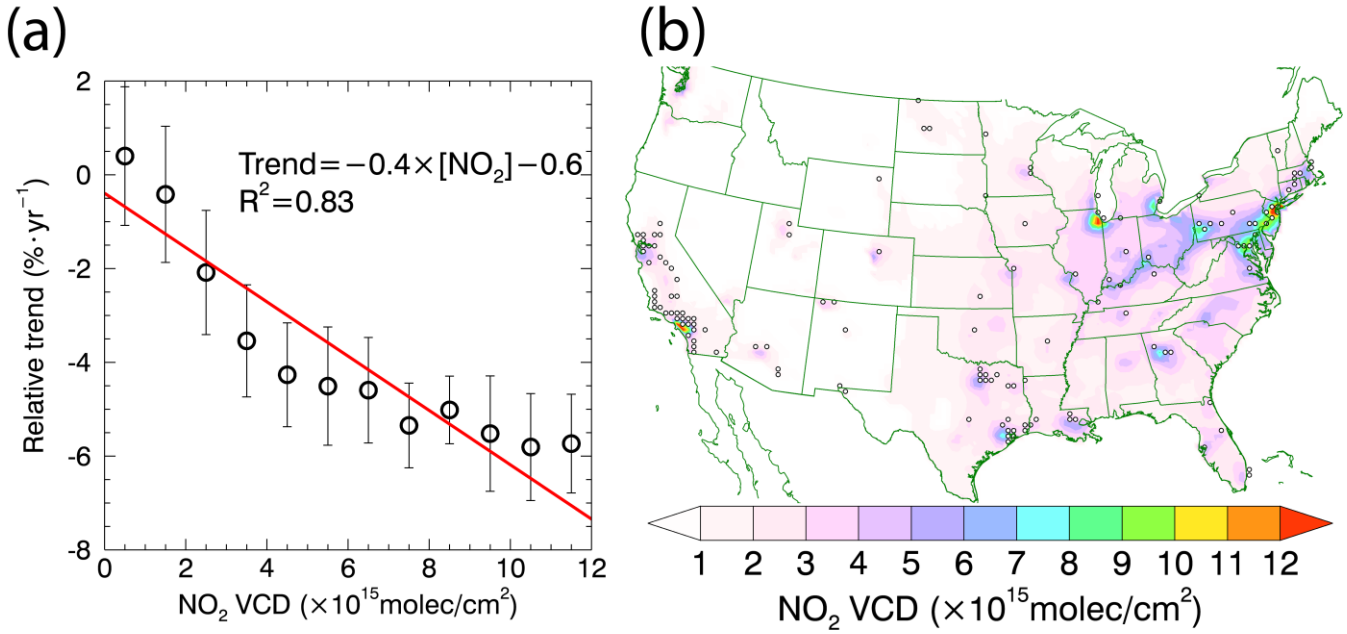

Figure 9. (a) The "Lightning filter" OMI-based NO_2 relative trend as a function 2005-2014 averaged OMI tropospheric NO_2 VCD binned every $1 \times 10^{15} molec/cm^2$. The error bars represent 95th percentile confidence intervals. The red line shows a least-squares regression. (b) The distribution of 2005-2014 averaged OMI tropospheric NO_2 VCD. Black bordered circles represent AQS sites. The ~~corrected~~ OMI tropospheric NO_2 data ("Lightning filter") are used.

Table 1. Annual relative trends calculated with coincident data and all available data. The 95th percentile confidence intervals from Mann-Kendall method are also listed.

Region	Annual relative trends of coincident data (% yr^{-1})				Annual relative trends using all data (% yr^{-1})			
	Standard		Lightning filter[a]		Standard		Lightning filter	
	AQS	OMI	AQS	OMI	AQS	OMI[b]	AQS	OMI[b]
West	-4.1±0.5	-3.2±0.4	-4.2±0.5	-3.8±0.4	-4.1±0.5	-0.9±0.4	-4.2±0.5	-2.0±0.3
Midwest	-3.4±0.5	-3.6±0.4	-2.8±0.6	-3.1±0.5	-2.5±0.5	-0.9±0.4	-2.2±0.5	-1.8±0.4
Northeast	-5.8±0.5	-5.0±0.5	-5.2±0.6	-5.3±0.7	-4.7±0.5	-3.0±0.4	-4.1±0.5	-3.1±0.5
South	-3.8±0.4	-2.7±0.3	-3.0±0.5	-3.0±0.5	-3.5±0.4	-0.2±0.4	-3.0±0.5	-0.9±0.3
Nationwide	-4.3±0.4	-3.5±0.3	-4.1±0.4	-3.9±0.3	-4.0±0.4	-0.7±0.3	-3.9±0.4	-1.5±0.2

[a] These data include the three ~~corrections~~data processing procedures of this study, namely, ocean trend correction, MODIS albedo update, and lightning filter screening.

[b] The spatial coverage is shown in Figure 1.